AD_____

Award Number: DAMD17-01-1-0463

TITLE: Outcome Based Screening for Prognostic Phospho-RTK (Receptor Tyrosine Kinase) Antibodies Using Tissue Microarrays

PRINCIPAL INVESTIGATOR: David Rimm, M.D., Ph.D.

CONTRACTING ORGANIZATION: Yale University
New Haven, Connecticut 06520-8047

REPORT DATE: August 2004

TYPE OF REPORT: Final

PREPARED FOR: U.S. Army Medical Research and Materiel Command
Fort Detrick, Maryland 21702-5012

REPORT DOCUMENTATION PAGE

Form Approved
OMB No. 074-0188

1. AGENCY USE ONLY (Leave blank)	2. REPORT DATE	3. REPORT TYPE AND DATES COVERED
	August 2004	Final (1 Aug 2001 - 31 Jul 2004)

4. TITLE AND SUBTITLE
Outcome Based Screening for Prognostic Phospho-RTK (Receptor Tyrosine Kinase) Antibodies Using Tissue Microarrays

5. FUNDING NUMBERS
DAMD17-01-1-0463

6. AUTHOR(S)
David Rimm, M.D., Ph.D.

7. PERFORMING ORGANIZATION NAME(S) AND ADDRESS(ES)
Yale University
New Haven, Connecticut 06520-8047

E-Mail: David.rimm@yale.edu

8. PERFORMING ORGANIZATION REPORT NUMBER

9. SPONSORING / MONITORING AGENCY NAME(S) AND ADDRESS(ES)
U.S. Army Medical Research and Materiel Command
Fort Detrick, Maryland 21702-5012

10. SPONSORING / MONITORING AGENCY REPORT NUMBER

11. SUPPLEMENTARY NOTES
Original contains color plates: All DTIC reproductions will be in black and white.

12a. DISTRIBUTION / AVAILABILITY STATEMENT
Approved for Public Release; Distribution Unlimited

12b. DISTRIBUTION CODE

13. ABSTRACT (Maximum 200 Words)

Receptor Tyrosine Kinases (RTKs) have been identified as potential targets for both breast cancer prognosis and therapy. We proposed use of tissue microarrays to evaluate the prognostic value of RTKs with emphasis on the phosphorylation status of these receptors. Analysis of a series of phospho-receptor antibodies on large cohorts on tissue microarrays should reveal which RTKs are most likely to be of prognostic and therapeutic value. As of this progress report, we have completed construction of the tissue microarrays and completed collection of the clinical data. We have also completed and submitted a pilot study of RTKs using conventional analysis of this array. In the proposal we show automated analysis of the arrays has potential to reveal relationships that are undetectable by conventional methods. We have now completed our efforts in construction of the device capable of high through-put automated array analysis. We have completed studies using this technology (called AQUA, for automated quantitative analysis)on a number of RTKs. Although we were unable to successfully use phosphor-Ab, the quantitative assess of the RTKs themselves provided novel information with respect

14. SUBJECT TERMS
No subject terms provided.

15. NUMBER OF PAGES
43

16. PRICE CODE

17. SECURITY CLASSIFICATION OF REPORT	18. SECURITY CLASSIFICATION OF THIS PAGE	19. SECURITY CLASSIFICATION OF ABSTRACT	20. LIMITATION OF ABSTRACT
Unclassified	Unclassified	Unclassified	Unlimited

Table of Contents

Introduction:

Biologically specific therapies represent a great new hope for combating cancer. Perhaps the best example of this is Herceptin, a specific drug for a subset of patients with HER2 positive breast cancer. Unfortunately, the pathway from initial discovery to clinical usage is long and slow, taking over 10 years for HER2 (a member of the receptor tyrosine kinases (RTK) family. In this study we proposed a potential method for rapid evaluation of other RTKs as bio-specific therapies based on prediction of outcome. We proposed that phospho-specific antibodies to RTK would provide highly specific prognostic markers for outcome and predictive markers for response to anti-receptor type therapies. Our objective was to produce specific phospho-RTK antibodies and then to evaluate them using breast cancer tissue microarrays. Breast cancer tissue microarrays are a method of placing 0.6 mm diameter samples of breast cancers from hundreds of patients on a single slide. Using this method we proposed high throughput screening for potential prognostic antibodies at the earliest stages of antibody development.

Body:

The main difficulty in finding these potential new RTK targets is that there are many potential candidates and it is difficult and expensive to evaluate a large number of antibodies on large breast cancer cohorts using conventional methods. The novelty or "idea" of this proposal is the use of a newly described, high throughput mechanism for evaluation of antibodies. Thus instead of producing candidate antibodies and screening using the conventional approach (which can take many years), we propose reversal of this process, screening for candidates using the outcome testing, then only proceeding with development of antibodies that have already been validated on large populations of breast cancer patients. We originally proposed the following specific aims:

1. Construction of a series of candidate phospho-RTK antigens and immunization into mice.
2. Evaluation of mouse test bleeds using 250 case, 3-fold redundant, breast cancer cohort tissue microarrays.
3. Selection of promising sera and production of monoclonal antibodies followed by confirmatory testing on tissue microarrays.

Our original Statement of Work was as follows:

Year 1:

1. Select and produce phospho- and corresponding non-phospho-peptides representing critical sequences of RTKs
2. Select 250 breast cancer cases and begin construction of tissue microarray
3. Inoculate mice with first set of phospho-peptides and collect test bleeds.
4. Begin first array screening

Year 2

1. Collect test bleeds and screen arrays.
2. Do final inoculations and test bleeds

3. Begin full scale TMA verification of first promising candidates
4. Do fusions and begin production of first Mabs
5. Production of small scale cloning verification tissue microarrays

Year 3

1. Complete production of Mabs
2. Complete verification of Mabs using first small scale TMAs
3. Production and large cohort testing (750+ case) of new antibodies

This progress report describes work completed during the three year duration of this grant.

In evaluation of the optimal RTKs for antibody preparation we consulted many sources. We found that many biotech antibody companies had already embarked on production of phospho-specific and other RTK antibody production. Rather that try to duplicate their efforts, we decided to begin by purchasing some of the 100's of RTK antibodies that are now commercially available.

Prior to testing any antibodies, arrays needed to be constructed and cohort data collected. That process was completed during the first year. We now have constructed 3 master array blocks for analysis. They include YTMA10 , including 350 node positive cases, YTMA 12, including 350 node negative cases, and YTMA 23, including a total of 250 cases representing a subset of the previous cohorts (125 node negative and 125 node positive) that have ample tissue available for analysis of multiple antibodies. During the analysis of YTMA 10 and 12 we found some slide to slide variability, such that is would be advantageous to mix the node positives (YTMA10) with the node negative (YTMA 12). This was done and produced as YTMA-49. This array was used extensively for studies on the RTKs.

After completion of construction of the arrays, we began a two-fold approach to analysis. As a proof of concept, we selected 5 RTKs (HER2, MET, EGFR, FGFR, and IGFR) as test cases. Dr. Tolgay Ocal, a pathologist recruited to this effort, analyzed expression of these markers using YTMA 12. He found that only Met was predictive of outcome in the node-negative population but that we were able to group MET and FGFR in a single group that was unrelated to HER2 and EGFR which comprised a second, unrelated group. Furthermore, he found that the localization of the epitope on Met was critical for prognostication of outcome. Specifically, the C-terminal antibody (3D4) was significantly associated with poor outcome, but a second antibody recognizing the extra-cellular domain of the Met beta chain was not at all associated with outcome. This was confirmed in a second effort using the same array looking at Met, matriptase, HAI 1 and HGF led by Julie Kang. Both of these efforts have now been published and both papers are included in the appendix.

Although we were pleased with these results, the original grant discussed analysis of arrays using a more quantitative method than the ordinal subjective scale used in this study. Toward that aim, other investigators in the lab have finalized a method for automated quantitative analysis of tissue microarrays. This work will be extremely valuable in optimizing the high throughput analysis of arrays in the future. Although the automated analysis development work was not funded by this grant, it impacts the grant dramatically. The paper that describes the new automated analysis system (AQUA) was published in Nov 2002 in Nature Medicine. That technology has now been used on a series of RTKs.

The automated analysis system was designed on the Applied Precision Deltavision platform, but that platform is not well suited to the task and the system at our institution is very heavily used allowing only limited time for our applications. Approval of a rebudgeting request allowed the purchase of a new dedicated 2nd generation automated tissue microarray analysis device. This device (called Professor Marvel, in honor of its location behind the curtain) is functioning well and the basis for all automated analysis experiments.

The next step was the evaluation of multiple phospho-specific antibodies. Although we originally proposed making our own phospho-specific antibodies, since that proposal, many have become commercially available. Thus we have purchased a number of antibodies to the tyrosines proposed in the original grant. Over the last 2 years, we have focused on the phospho-tyrosines of Met, EGFR, and HER2. The antibodies were purchased from Cell Signaling Technologies (CST), Upstate Biochemical and Biosource. We collected data on all of the phospho-tyrosines on EGFR and all of the phosphor tyrosines of Met using the 250 case TMA. These antibodies have shown some unexpected subcellular localizations (specifically many are nuclear). This has led to questions regarding antibody cross reactivity or non-specificity.

This led to validation studies of three Phospho-Met antibodies from BioSource. Although these are not monoclonals, they are made from three phospho-peptides (Y1003, Y1235, and Y1349), and then affinity purified. Others and we have shown these antibodies work on western blots by showing increased phosphorylation after stimulation with HGF, the Met ligand. However, the patterns on test arrays were variable from case to case and the localization was not similar to that seen with some Met antibodies. Toward validation of these antibodies, first we used incubation with phosphatases to determine if the antigens are destroyed. We found that Calf Intestinal Alkaline Phosphatase was sufficient to abolish essentially all activity of the phospho-Met antibodies. Next we tested the specificity of each of the three phospho-met antibodies by using purified phospho-peptides to assess competitive inhibition of the interactions on tissue arrays. Figure 1 shows that the Y1349 antibody is somewhat diminished (row 3) or barely at all diminished (row 1) by the phospho-Y1349 peptide, but it is similarly competed by the phospho-Y1003 and Y1235 peptides. We conclude that even though there is specificity on a western blot, on fixed tissue there is significant cross-reactivity that will prevent future use of these antibodies in this project.

Although were are still concerned about the heterogeneity of phosphorylation, we plan to proceed to test further phospho-specific monoclonal antibodies, beginning with the Cell Signaling Technologies phospho-EGFR antibodies. Over the last year Julie Kang and Matt Neopolitano tested phosphor-EGFR and phosphor-met antibodies on YTMA 23 (the 250 case cohort). These studies showed disappointing results in multiple ways. Initially data analysis showed that all markers analyzed showed no relationship to outcome. While Tyr 845 of EGFR trended toward significance, the data was disappointing. Further analysis suggested two main problems that lead to abandonment of this strategy. Firstly, we found heterogeneity it the phosphor-specific antibodies that was not seen with other antibodies, raising the possibility that variation in phosphatase activity prior to fixation may represent a fatal flaw in the cohort. We had no way to control for this variable since the tissue was collected from archival material from many years ago. The second major problem was a incompatibility in the amplification scheme. We found that the membrane compartmentalization marker that was used (ConA) caused increased background, most likely due to interaction with the dextran backbone in the Envision™ kit used for measuring the target in the AQUA system.

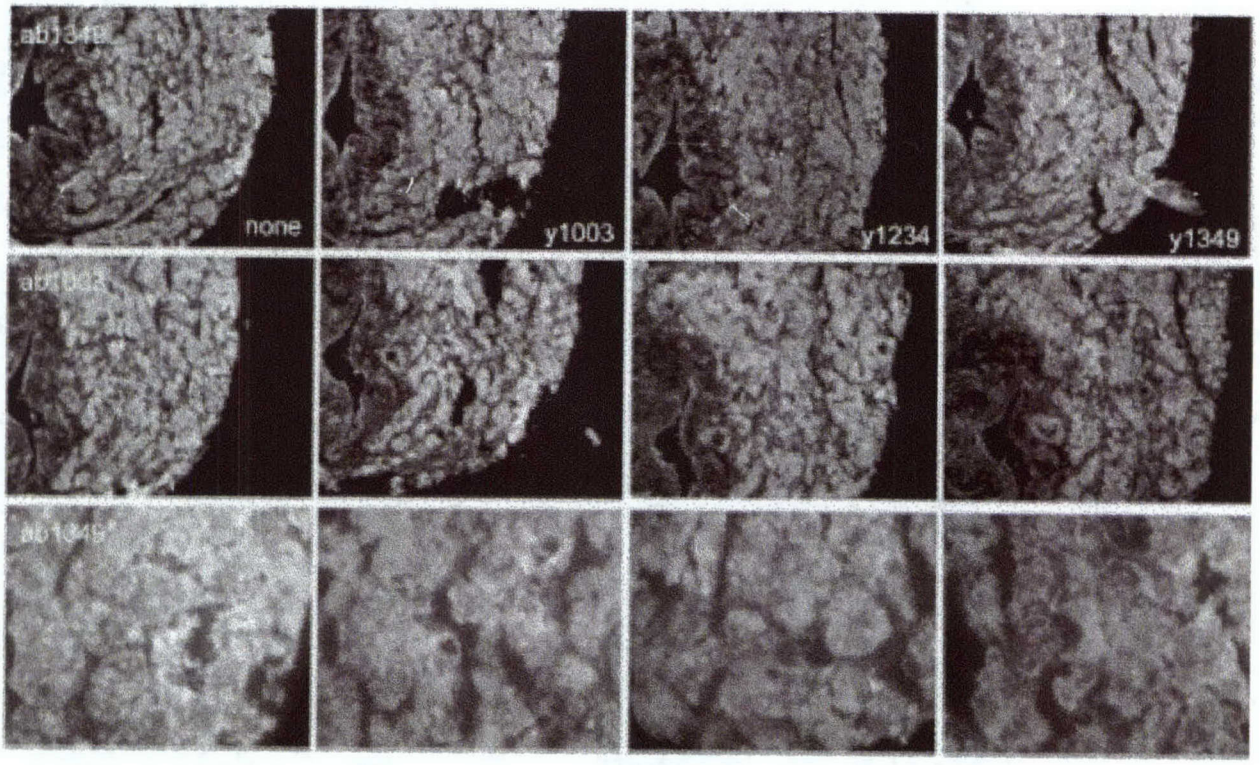

Figure 1: Competition assays of phospho-specific antibodies by phospho-peptides show non-specific peptides are as effective as specific peptides for competition in immunofluorescence assays. Rows 1 and 3 are the antibody to Y1349 of the cytoplasmic domain of Met, shown at 20X and 40X respectively. Row 2 is the Y1003 antibody. Row 1 shows the phospho-peptide

used for each column of images: column 1, none; column 2, Y1003; column 3, Y1234; column 4 Y1349.

Given this series of problems and some changes in personnel, we decided to focus more on the HER family molecules themselves in preparation for analysis to look at dimerization and or co-localization with downstream binding partners. This work was done by a new MD-PhD student that entered the lab, Jena Giltnane. She has found that different EGF antibodies show highly variable patterns and levels of expression dependent on the epitope (see figure 2). The Dako antibody showed borderline significance in prediction of outcome, while the CST antibody showed no relationship to outcome. The data in preliminary and will be repeated to increase the spot redundancy. Jena has also done a preliminary analysis comparing expression levels between the other HER family molecules. This is the subject of a new Army Idea grant submitted last June.

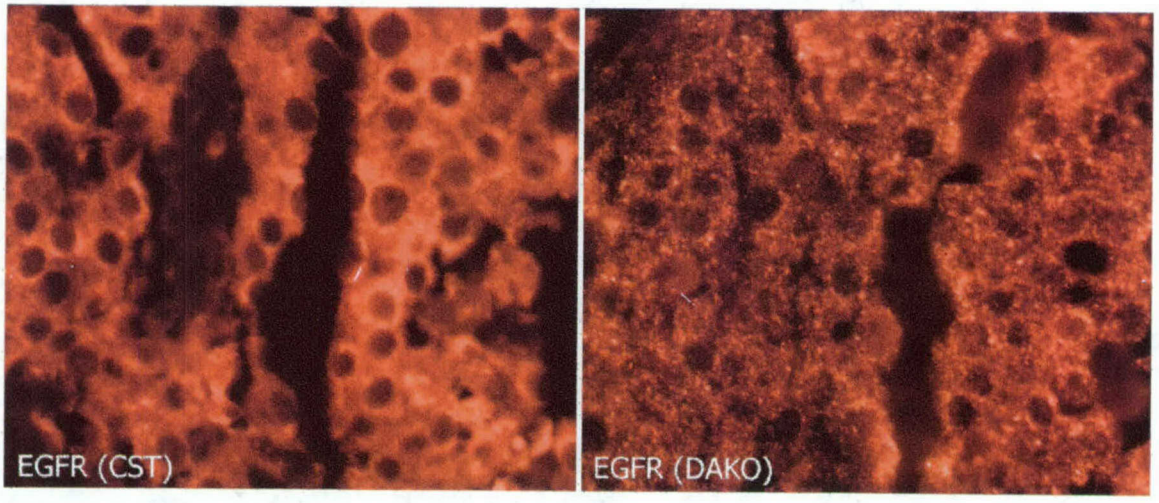

Figure 2: Serial sections of the same tumor section stained overnight with DAKO (extracellular) and Cell Signaling Technologies (intracellular) antibodies to EGFR. The CST antibody has been used without significant results on breast and colon arrays; the FDA-approved companion diagnostic for EGFR targeted therapy is a DAKO antibody. Staining conditions were identical.

Key Research Accomplishments:

- Completion of technology for high throughput automated analysis of tissue microarrays
- Completion of array construction of both the 250 case array and the 700 case array and cohort

- Completion of RTK conventional pathologist-based analysis of array with node negative cohort
- Testing of phospho-specific antibodies on arrays
- AQUA based automated analysis of EGFR antibodies

Reportable Outcomes:

Analysis of RTKs shows MET is predictive of outcome in a node-negative population and it identifies a series of patients unique from that identified by over-expression of HER2 or EGFR but related to those that over-express FGFR.

Conclusions:

Tissue microarrays are a valuable tool for analysis of protein and phospho-protein expression. Completion of our automated analysis system will allow high throughput analysis of these arrays. We have further developed and system for quantitative analysis of these arrays. We have now switched over to exclusively using this AQUA technology.

The significance of these developments is that we are now well positioned to find a series of valuable prognostic markers. Although phosphor-specific antibodies were a disappointment due to uncontrollable issues in the fixation process, the antibodies to the RTKs themselves have been measured in a quantitative manner and we have show that different regions of the molecule show different staining patterns and different associations with outcome. These markers and their downstream binding partners are likely to be valuable for prognostication and prediction as the number of RTK specific drugs increases.

References:

See original proposal.

Appendices:

1. Camp, R.L. Chung, G.G., and Rimm, D.L. (2002) *Algorithms for Automated Tissue Microarray Analysis Reveal Novel Disease Sub-classifications.* Nature Medicine 8(11):1323-8

2. Kang, J.Y., Dolled-Filhart, M.,. Ocal, I.T., Singh, B., Lin, C-Y., Dickson, R.B., Rimm, D.L. and Camp, R.L. (2003) *Tissue Microarray Analysis of Hepatocyte Growth Factor/Met Pathway Components Reveals a Role for Met, Matriptase, and Hepatocyte Growth Factor Activator Inhibitor 1 in the Progression of Node-negative Breast Cancer.* Cancer Research 63:1101-1105.

3. Ocal, I.T., Dolled-Filhart, M.P, D'Aquila, T.G., Camp, R.L. and Rimm, D.L (2003) *Tissue Microarray based studies of node-negative breast cancer patients show Met expression associated with worse outcome but not correlated with EGF family receptors.* Cancer 97(8):1841-1848.

4. Camp, R.L., Dolled-Filhart, King, B and Rimm, D.L. (2003) *Quantitative Analysis of Breast Cancer Tissue Microarrays Shows That Both High and Normal Levels of HER2 Expression Are Associated with Poor Outcome.* Cancer Research 63:1445-1448.

OUTCOME BASED SCREENING FOR PROGNOSTIC PHOSPHO-RTK ANTIBODIES USING TISSUE MICROARRAYS

AWARD NUMBER DAMD17-01-1-0463

PI: DAVID L. RIMM, M.D., Ph.D.

TABLE OF CONTENTS

1. Camp, R.L. Chung, G.G., and Rimm, D.L. (2002) *Automated subcellular localization and quantification of protein expression in tissue microarrays..* Nature Medicine 8(11):1323-7

2. Kang, J.Y., Dolled-Filhart, M.,. Ocal, I.T., Singh, B., Lin, C-Y., Dickson, R.B., Rimm, D.L. and Camp, R.L. (2003) *Tissue Microarray Analysis of Hepatocyte Growth Factor/Met Pathway Components Reveals a Role for Met, Matriptase, and Hepatocyte Growth Factor Activator Inhibitor 1 in the Progression of Node-negative Breast Cancer.* Cancer Research 63:1101-1105.

3. Ocal, I.T., Dolled-Filhart, M.P, DíAquila, T.G., Camp, R.L. and Rimm, D.L (2003) *Tissue Microarray based studies of node-negative breast cancer patients show Met expression associated with worse outcome but not correlated with EGF family receptors.* Cancer 97(8):1841-1848.

4. Camp, R.L., Dolled-Filhart, King, B and Rimm, D.L. (2003) *Quantitative Analysis of Breast Cancer Tissue Microarrays Shows That Both High and Normal Levels of HER2 Expression Are Associated with Poor Outcome.* Cancer Research 63:1445-1448.

Automated subcellular localization and quantification of protein expression in tissue microarrays

ROBERT L. CAMP, GINA G. CHUNG & DAVID L. RIMM

Department of Pathology, Yale University School of Medicine, New Haven, Connecticut, USA

Correspondence should be addressed to D.L.R.; email: david.rimm@yale.edu

Published online 21 October 2002; doi:10.1038/nm791

The recent development of tissue microarrays—composed of hundreds of tissue sections from different tumors arrayed on a single glass slide—facilitates rapid evaluation of large-scale outcome studies. Realization of this potential depends on the ability to rapidly and precisely quantify the protein expression within each tissue spot. We have developed a set of algorithms that allow the rapid, automated, continuous and quantitative analysis of tissue microarrays, including the separation of tumor from stromal elements and the sub-cellular localization of signals. Validation studies using estrogen receptor in breast carcinoma show that automated analysis matches or exceeds the results of conventional pathologist-based scoring. Automated analysis and sub-cellular localization of beta-catenin in colon cancer identifies two novel, prognostically significant tumor subsets, not detected by traditional pathologist-based scoring. Development of automated analysis technology empowers tissue microarrays for use in discovery-type experiments (more typical of cDNA microarrays), with the added advantage of inclusion of long-term demographic and patient outcome information.

Despite the promise of automated analysis of histological sections, it has failed to replace traditional, pathologist-based evaluation, even in the simplest of conditions such as the analysis of immunohistochemical stains. Whereas the automated analysis of isolated cells in fluids or smears (for example, fluorescent cell sorting and laser scan cytometry) is now routine[1], the analysis of tissue sections is hampered by the fact that tumor tissue is a complex mixture of overlapping malignant tumor cells, benign host-derived cells and extracellular material. Several methods (including confocal and convolution/deconvolution microscopy) can determine the subcellular localization of target antigens, but only through computationally intensive techniques, requiring the acquisition of multiple high-power, serial images[2]. Methods designed for tissue microarrays perform only limited subcellular localization using morphometry and usually require significant manual interface (for example, drawing polygons around tumor cells)[3,4]. In general, pathologist-based analysis remains the current standard for the immunohistochemical studies.

Tissue microarrays provide a high-throughput method of analyzing the prognostic benefit of a myriad of potential targets on large cohorts of patient samples[5–7], but are limited by the pathologist's ability to reproducibly score on a continuous scale, discriminate between subtle low-level staining differences, and accurately score expression within subcellular compartments. We have developed a set of algorithms that we call AQUA (Automated Quantitative Analysis) that allow the rapid, automated analysis of large-scale cohorts on tissue microarrays. The first algorithm, called PLACE (pixel-based locale assignment for compartmentalization of expression) utilizes fluorescent tags to separate tumors from stroma and to define subcellular compartments. The distribution of a target antigen is then quantitatively assessed according to its co-localization with these tags. As subcellular compartments (for example, membrane, cytoplasm, nuclei and so forth) of different tissues and tumors vary widely in size and shape, traditional methods of defining compartments based on morphometric criteria (that is, feature extraction) perform poorly on a large-scale basis. Rather than counting target-containing features, PLACE delineates target expression as the sum of its intensity divided by the total size of the assayed compartment.

As the thickness of tissue sections makes it difficult to discriminate between overlapping subcellular compartments, we have also developed a novel, rapid exponential subtraction algorithm (RESA), which subtracts an out-of-focus image, collected slightly below the bottom of the tissue, from an in-focus image, based on pixel intensity, signal-to-noise ratio, and the expected compartment size. This algorithm dramatically improves the assignment of pixels to a particular subcellular compartment (Fig. 1). For a more complete discussion of the image manipulations performed in this protocol, see Supplementary Methods or http://www.yalepath.org/dept/research/YC-CTMA/tisarray.htm.

Validation of AQUA algorithms

Our initial validation of this technology compared its accuracy, intra-observer variability, and predictive power to traditional pathologist-based analysis. We stained a tissue microarray derived from 340 node-positive breast-carcinoma patients for the presence of estrogen receptor (ER)—the oldest and most common prognostic marker for breast cancer[8]. First we analyzed the ability of automated analysis to match results from a pathologist-based evaluation and found a high degree of correlation ($R = 0.884$, Fig 2*a*). Next, we compared the variability of a pathologist-based and automated analysis of two separate histospots derived from the same tumor (Fig. 2*b* and *c*). This comparison shows that automated analysis has slightly better reproducibility ($R = 0.824$ versus $R = 0.732$).

Although automated analysis compares favorably with pathologist-based interpretation of microarrays, the true criterion standard is outcome prediction. Estrogen receptor expression is known to significantly improve outcome, because it is associated with less aggressive tumors that are more responsive to anti-estrogenics (for example, Tamoxifen). We compared the survival of patients with tumors with high (top 25%) versus low (bottom 25%) ER expression as assessed by both automated and pathologist-based scoring (Fig. 2*d*). Results show that both methods provide similar prognostic information (*RR* = 2.44 versus 2.06, automated versus pathologist); although the auto-

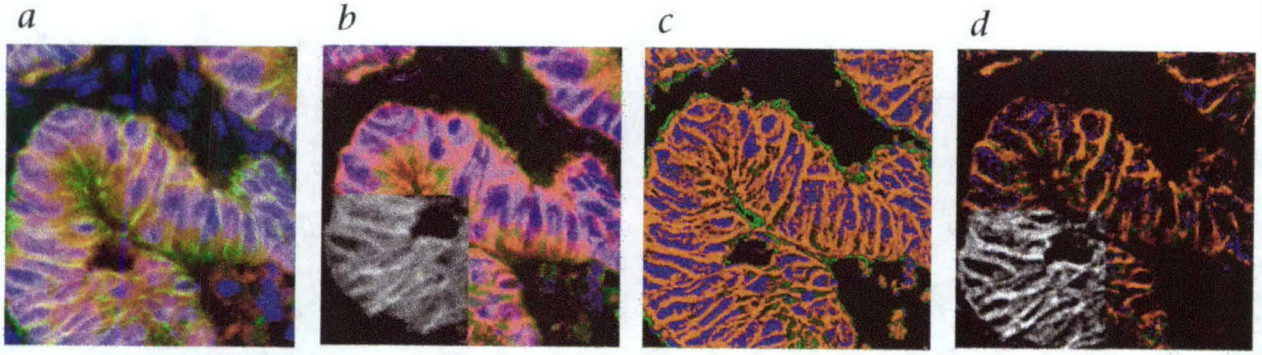

Fig. 1 RESA allows the accurate assignment of subcellular compartments and localization of a target antigen. ***a***, A pseudo three-color image of a colon carcinoma shows a significant degree of overlap between subcellular compartments: Blue, nuclei (DAPI); green, tumor mask (cytokeratin); red, tumor cell membranes (alpha-catenin). ***b***, The signal intensity of a target antigen, β-catenin (inset), is redistributed according to the relative signal intensity of the compartments identified in *a*: Blue, nuclear-localized; red, membrane-localized; green, cytoplasmic. Note that the β-catenin expression in this tumor is predominantly membrane-associated, yet there is significant incorrectly assigned signal in the nucleus: magenta and blue pixels. ***c***, The compartment-specific signals in *a* are reassigned using the RESA algorithm, reducing the amount of overlapping signal by exponentially subtracting pixel intensity from an out-of-focus image. ***d***, The signal intensity from an exponentially subtracted image of the target antigen, β-catenin (inset) is then redistributed according to the compartments defined in *c*. This results in more accurate assignment of the target antigen to the membrane compartment (red pixels) with little expression in the nuclear compartment (blue pixels).

mated analysis shows slightly higher significance ($P = 0.0003$ versus $P = 0.0020$). Univariate analysis of the automated analysis shows a relative risk of 2.438 ($P = 0.0005$, 95% CI 1.480–4.016). When analyzed in a multivariate analysis against histological and nuclear grades, age and stage, automated ER analysis retains independent prognostic significance ($RR = 2.566$, 95% CI 1.428–4.611, $P = 0.0016$). The pathologist-based analysis shows similar results, validating the cohort (see Supplementary Methods).

To determine the reproducibility of our automated analysis of ER, we used the 'split-sample technique,' by dividing the cohort into halves and using one half as a 'training' set and the other as a 'test' set[9]. The training set was used to determine standard cutoffs for the top and bottom 25% of cases. These cutoffs were then used to divide the test set into top, middle and bottom groups. We analyzed 300 randomly selected training and test sets; on average 97% of the test cases were correctly classified.

One clear advantage to automated analysis is that it can perform a true continuous assessment of a target. In contrast, the human eye, even that of a trained pathologist, has a difficult time accurately distinguishing subtle differences in staining intensity using a continuous scale. Consequently, scoring systems for pathologists tend to be nominal (for example, 0, 1+, 2+, 3+). Algorithms such as the 'H-score' are meant to translate such nominal observations into semi-quantitative results. However, the inability to detect subtle differences in staining intensity, particularly at the low and high ends of the scale, as well as the tendency to round scores limits the effectiveness of the H-score. The discontinuity of pathologist-based scoring, despite the use of an H-score algorithm, is exemplified in the

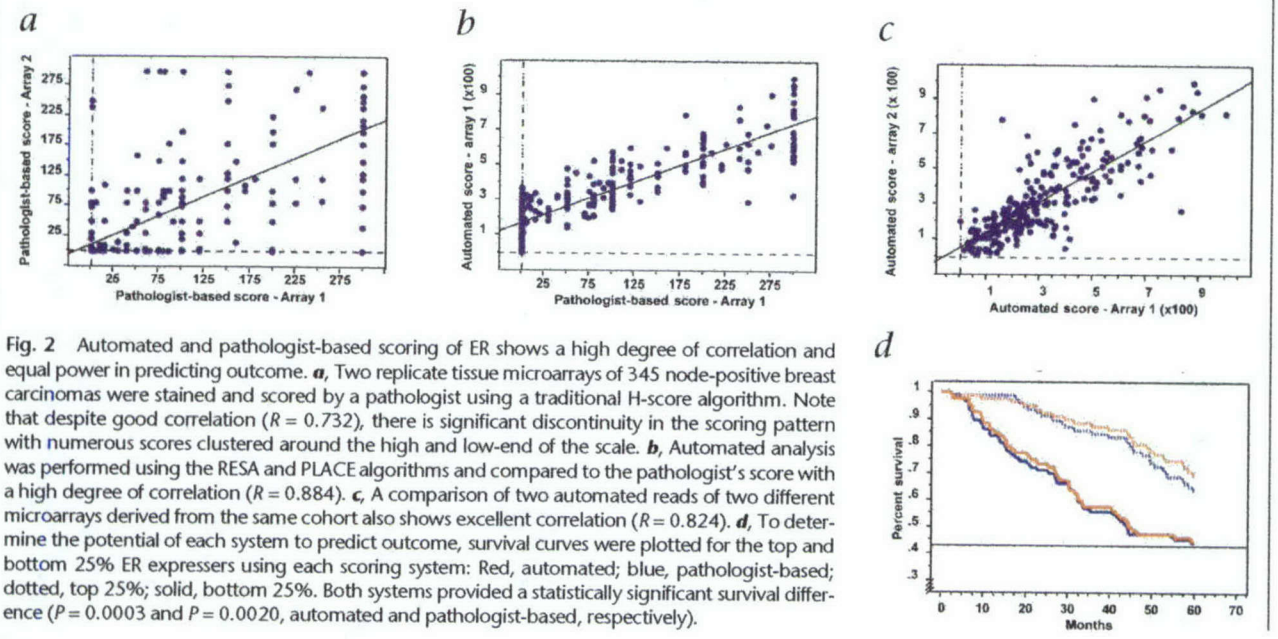

Fig. 2 Automated and pathologist-based scoring of ER shows a high degree of correlation and equal power in predicting outcome. ***a***, Two replicate tissue microarrays of 345 node-positive breast carcinomas were stained and scored by a pathologist using a traditional H-score algorithm. Note that despite good correlation ($R = 0.732$), there is significant discontinuity in the scoring pattern with numerous scores clustered around the high and low-end of the scale. ***b***, Automated analysis was performed using the RESA and PLACE algorithms and compared to the pathologist's score with a high degree of correlation ($R = 0.884$). ***c***, A comparison of two automated reads of two different microarrays derived from the same cohort also shows excellent correlation ($R = 0.824$). ***d***, To determine the potential of each system to predict outcome, survival curves were plotted for the top and bottom 25% ER expressers using each scoring system: Red, automated; blue, pathologist-based; dotted, top 25%; solid, bottom 25%. Both systems provided a statistically significant survival difference ($P = 0.0003$ and $P = 0.0020$, automated and pathologist-based, respectively).

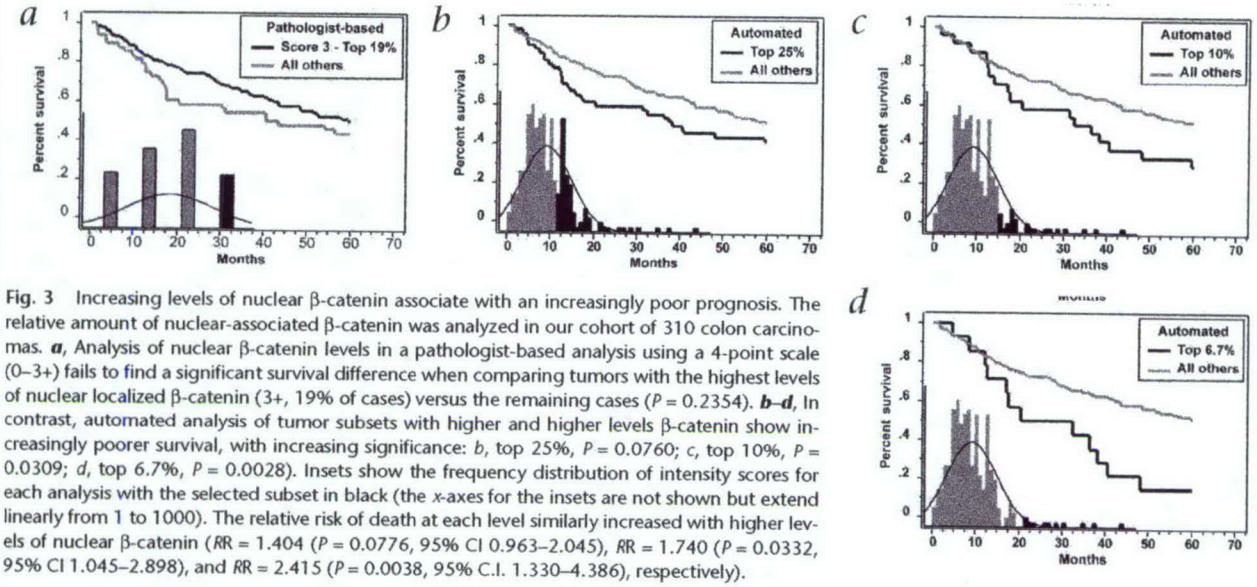

Fig. 3 Increasing levels of nuclear β-catenin associate with an increasingly poor prognosis. The relative amount of nuclear-associated β-catenin was analyzed in our cohort of 310 colon carcinomas. ***a***, Analysis of nuclear β-catenin levels in a pathologist-based analysis using a 4-point scale (0–3+) fails to find a significant survival difference when comparing tumors with the highest levels of nuclear localized β-catenin (3+, 19% of cases) versus the remaining cases ($P = 0.2354$). ***b–d***, In contrast, automated analysis of tumor subsets with higher and higher levels β-catenin show increasingly poorer survival, with increasing significance: *b*, top 25%, $P = 0.0760$; *c*, top 10%, $P = 0.0309$; *d*, top 6.7%, $P = 0.0028$). Insets show the frequency distribution of intensity scores for each analysis with the selected subset in black (the *x*-axes for the insets are not shown but extend linearly from 1 to 1000). The relative risk of death at each level similarly increased with higher levels of nuclear β-catenin (*RR* = 1.404 ($P = 0.0776$, 95% CI 0.963–2.045), *RR* = 1.740 ($P = 0.0332$, 95% CI 1.045–2.898), and *RR* = 2.415 ($P = 0.0038$, 95% C.I. 1.330–4.386), respectively).

ER staining results in Fig. 2. Note the preponderance of scores at 0, 100, 200 and 300. Furthermore, on average, over half of the cases were assigned to one extreme or the other (39% at 0 and 12% at 300). Thus 51% of the cases could not be effectively ranked. In contrast, the range of scores from the automated analysis is continuous from 0 to 1000. We hypothesize that the two key advantages of automated assessment, continuity of scoring and accurate subcellular localization, will allow tumor classification beyond that attainable by current methods.

Compartmental analysis of beta-catenin expression

To demonstrate this potential, we analyzed β-catenin expression in colon cancer. β-catenin is an ideal candidate in that it exhibits complex subcellular localization and manifests oncogenic properties upon localization to the nucleus[10]. Numerous studies have shown that β-catenin plays a dual role in both cell–cell adhesion and cell proliferation, depending on its location[11]. Membrane-associated β-catenin stabilizes cadherins-mediated adhesion by facilitating the cytoskeletal attachment of adhesion complexes. In contrast, nuclear-associated β-catenin activates several genes important in cell proliferation and invasion[12]. In development, translocation of β-catenin to the nucleus results from *wnt*-mediated cell signaling[13]. However, spurious activation of this pathway is often seen in tumors through mutation of β-catenin or other proteins involved in its activation and/or degradation[14]. Studies on the prognostic value of β-catenin have been mixed[15–17].

The complex biology and uncertain prognostic value of β-catenin made it a suitable candidate for assessing the value of quantitative subcellular localization. We studied a cohort of 310 colon cancers, using both pathologist-based and automated systems for scoring overall, nuclear and membrane-associated levels of β-catenin expression. Manual analysis used a traditional 4-point nominal scale (0 through 3+), whereas automated analysis used a continuous 1,000-point scale. In a previous study using a similar cohort, we were unable to find prognostic value in assessing nuclear β-catenin levels[18]. These data were confirmed in our present study when comparing tu-

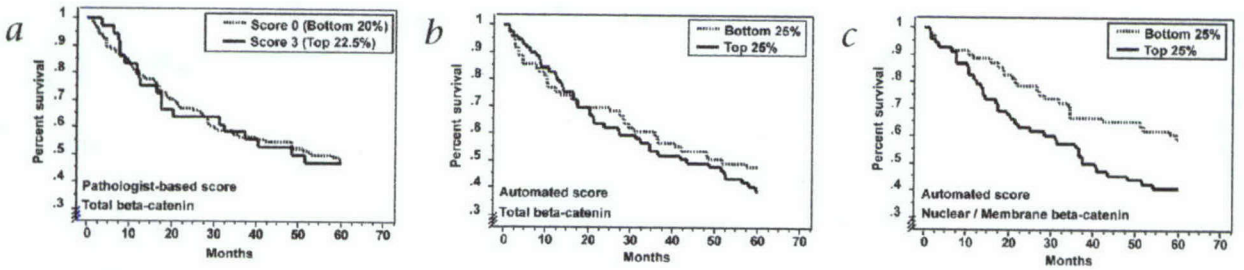

Fig. 4 Unlike analyses of overall β-catenin expression, automated, subcellular localization of β-catenin can predict outcome in colon carcinoma. ***a***, Overall β-catenin levels in a cohort of 310 colon cancers were evaluated by a pathologist using a 4-point scale (0–3+). Survival analysis of tumors with the lowest (0) versus highest (3+) overall β-catenin expression was not significant ($P = 0.9425$). ***b***, Similarly, automated analysis of overall β-catenin levels, comparing cases in the top and bottom 25%, failed to detect a survival difference ($P = 0.4551$). ***c***, In contrast, the ratio of nuclear to membrane β-catenin, as assessed by automated analysis, demonstrates that tumors with higher relative nuclear expression do worse than those with higher relative membrane expression ($P = 0.0264$, top versus bottom 25% of cases, *RR* = 1.718, 95% CI = 1.059–2.787). Note that the nuclear/membrane ratio identifies a large subset (25%) of tumors with poor prognosis, the majority of which are not identified by analyzing individual subcellular compartments. Indeed, comparison of tumors with high nuclear/membrane ratios (top 25%) versus those with high nuclear β-catenin (top 25%) shows that there is only 47% overlap.

mors expressing the highest levels of nuclear β-catenin (3+, representing 19% of the cases) versus the rest (Fig 3*a*) (P = 0.2354). We hypothesized that with the benefit of automated, continuous assessment, these 3+ cases could be subdivided into cases expressing very high versus high levels. We began by analyzing the top 25% of tumors expressing nuclear β-catenin, as assessed by automated analysis. This group shows a trend toward poorer survival (Fig 3*b*) (P = 0.0760). When we subset the tumors to assess the top 10% expressers, there is a statistically significant survival difference (Fig. 3*c*) (P = 0.0332, relative risk = 1.740). Further fractionation of the data reveals that the top 6.7% (15th percentile) exhibit even poorer survival with a higher statistical significance (Fig. 3*d*) (P = 0.0038, relative risk = 2.415). This analysis demonstrates the power of continuous automated assessment to define subsets of tumors not seen using standard pathologist-based assessment. Unlike β-catenin, subdividing ER into smaller and smaller subsets does not significantly alter its prognostic ability, suggesting that ER may be a truly continuous marker where no subpopulations exist.

Tumor classification using the AQUA algorithms

We then attempted a tumor classification based on comparative subcellular localization. As the translocation of β-catenin from the membrane to the nucleus is thought to correlate with transcriptional activation, we analyzed the ratio of nuclear to membrane-localized β-catenin. By its nature, this type of analysis is essentially impossible without continuous scoring. A crude measurement of overall β-catenin levels using either a pathologist-based or an automated system fails to demonstrate a significant difference in survival between the highest and lowest expressing tumors (Fig. 4, *a* and *b*, P = 0.9425 and P = 0.4551, respectively). In contrast, when we ratio the level of nuclear/membrane β-catenin, we find that tumors with a high ratio have a worse outcome than tumors with a low ratio (RR = 1.718, P = 0.0284). Note that this method defines a relatively large subset (25%) of tumors with poor prognosis, the majority of which are not identified by analyzing individual subcellular compartments. Indeed, a comparison of the tumors with the highest nuclear/membrane ratio (top 25%) versus the highest overall nuclear levels of β-catenin (top 25%) shows that there is only 47% overlap between the two subsets. Multivariate analysis of nuclear/membrane β-catenin ratios shows independent prognostic significance when analyzed with depth of invasion, nodal status, tumor grade and patient age (RR = 1.865, 95% CI = 1.068–3.259, P = 0.0285). In contrast, multivariate analysis of total nuclear β-catenin levels fails to show independent prognostic significance because it is highly correlated with nodal metastases (see Supplementary Methods online).

The methods presented here are highly adaptable to a number of tumor types and target markers. In most cases, compartment-specific tags are identical regardless of tumor type (DAPI for nuclei, cadherins/catenin complexes for membranes). Because the methods do not use heuristic models that require recognition of compartments according to size, shape or texture, they are fully adaptable to tumors with overlapping or pleomorphic cells and/or nuclei. Furthermore, the algorithms can be easily expanded to cover novel compartments or even 'virtual' compartments (for example, mitochondria, lysosomes, cortical actin ring) or tumor types (for example, mesothelioma), as long as tags can be identified for the prospective compartments/cell types. In addition to ER and β-catenin, we have used these techniques to successfully analyze dozens of markers, including growth factor receptors, intracellular signaling molecules, and proliferation markers, using both conventional and phospho-specific antibodies (see Supplementary Methods online). Analysis of these targets requires only a standard antibody titration.

We have found that most antigens benefit from subcellular localization. Localization can be simple, such as determining the amount of the proliferation marker KI-67 in tumor nuclei, or more complex as in the case of β-catenin. Localization of intracellular signaling molecules (for example, STATs) may be vital in assessing their potential as prognostic markers. In addition, recent studies have shown that membrane-bound growth factor receptors (for example, epidermal growth factors, EGFR and ERB-B4, and fibroblast growth factor) can translocate to the nucleus and may act as transcriptional regulators[19]. Subcellular localization of such markers may be critical to their use as prognostic markers in cancer.

Depending upon the array size, and the complexity of the compartmentalization, analyses using our current device take from 1–3 hours for image acquisition, and 1–2 hours for analysis. In our laboratory, the average pathologist-based analysis rate is 50–100 spots per hour and usually is performed in several sessions. To increase precision, two or more pathologists read the same array independently and then together to resolve discrepancies. Aside from being more accurate and more robust, automated analysis can be performed continuously and results tabulated immediately. We estimate that a fully integrated tissue microarray reader could be 30 to 50 times faster than pathologist-based scoring.

Methods

Tissue microarray design and processing. Paraffin-embedded formalin-fixed specimens from 345 cases of node-positive breast carcinoma (1962–1977) and 310 cases of colon carcinoma (1971–1982) were obtained, as available, from the archives of the Yale University Department of Pathology. Microarray slides were prepared, processed and stained as described in the Supplementary Methods online. For manual analysis, slides were visualized with diaminobenzidine (DAB). For automated analysis, slides were visualized with Cy-5 tyramide.

Image and data analysis. Monochromatic images of tissue microarray histospots were obtained using fluorescently labeled compartment specific tags (anti-cytokeratin, DAPI, α-catenin) as well as target signals (ER and β-catenin). Regions of tumor were identified using a mask derived from a ubiquitously expressed epithelial-specific antigen (either cytokeratin or α-catenin). Images were analyzed using RESA and PLACE algorithms as detailed in the Supplementary Methods online. Results were expressed as the intensity of the target signal in each compartment divided by the compartment. For ER, only nuclear-localized signal was used; for β-catenin total signal, the ratios of nuclear-to-membrane signal and nuclear-to-total signal were analyzed. Overall survival analysis was assessed using Kaplan–Meier analysis and the Mantel–Cox log-rank score for assessing statistical significance. Relative risk was assessed using the univariate and multivariate Cox-proportional hazards model.

Our data show that quantitative, continuous-scale, compartmentalized automated analysis of tissue microarrays can provide a rapid assessment of prognosis-based subsets in a variety of tumor markers that cannot be attained using pathologist-based techniques. Automated analysis is better able to discern subtle differences in staining intensity, particularly at the upper and lower extremes, which can distinguish novel prognostic associations. Furthermore, analysis of the subcellular distribution of certain signals, using the PLACE and RESA algorithms may elucidate previously unrecognized associations with patient survival. The automated nature of this technology can allow high-throughput screening of tissue microarrays, facilitating their use in large-scale, high-throughput applications such as target discovery and prognostic marker validation. If, someday, diagnostic criteria are based on molecular expression patterns, the digital nature of this analysis could allow a device of this type to make specific molecular diagnoses.

Note: Supplementary information available on the Nature Medicine *website.*

Acknowledgments

We thank T. D'Aquila, M. Helie, L. Charette, D. Fischer, E. Rimm and P. Lizardi for their help in this effort; and J. Costa, V. Marchesi, A. Reynolds, R. Levenson and E. Fearon for review of the manuscript. This work was supported by grants from the Patrick and Catherine Weldon Donaghue Foundation for Medical Research and grants from the NIH including: K0-8 ES11571, NIEHS (to R.L.C.), RO-1 GM57604 NCI (to D.L.R.) and US Army DAMD grant 01-000436.

Competing interests statement

The authors declare competing financial interests: see the website (http://nature.com/naturemedicine

1. Tarnok, A. & Gerstner, A.O. Clinical applications of laser scanning cytometry. *Cytometry* **50**, 133–143 (2002).
2. Robinson, J.P. Principles of confocal microscopy. *Methods Cell Biol.* **63**, 89–106 (2001).
3. Rao, J., Seligson, D. & Hemstreet, G.P. Protein expression analysis using quantitative fluorescence image analysis on tissue microarray slides. *Biotechniques* **32**, 924–932 (2002).
4. Bacus, S. *et al.* Potential use of image analysis for the evaluation of cellular predicting factors for therapeutic response in breast cancers. *Anal. Quant. Cytol. Histol.* **19**, 316–328 (1997).
5. Kallioniemi, O.P., Wagner, U., Kononen, J. & Sauter, G. Tissue microarray technology for high-throughput molecular profiling of cancer. *Hum. Mol. Genet.* **10**, 657–662 (2001).
6. Kononen, J. *et al.* Tissue microarrays for high-throughput molecular profiling of tumor specimens. *Nature Med.* **4**, 844–847 (1998).
7. Rimm, D.L. *et al.* Tissue microarray: a new technology for amplification of tissue resources. *Cancer J* **7**, 24–31 (2001).
8. Osborne, C.K. *et al.* Estrogen receptor, a marker for human breast cancer differentiation and patient prognosis. *Adv. Exp. Med. Biol.* **138**, 377–385 (1981).
9. Wasson, J.H., Sox, H.C., Neff, R.K. & Goldman, L. Clinical prediction rules. Applications and methodological standards. *N. Engl. J. Med.* **313**, 793–799 (1985).
10. Kobayashi, M. *et al.* Nuclear translocation of β-catenin in colorectal cancer. *Br. J. Cancer* **82**, 1689–1693 (2000).
11. Provost, E. & Rimm, D.L. Controversies at the cytoplasmic face of the cadherin-based adhesion complex. *Curr. Opin. Cell Biol.* **11**, 567–572 (1999).
12. Morin, P.J. β-catenin signaling and cancer. *Bioessays* **21**, 1021–1030 (1999).
13. Peifer, M. & Polakis, P. Wnt signaling in oncogenesis and embryogenesis—a look outside the nucleus. *Science* **287**, 1606–1609 (2000).
14. Wong, C.M., Fan, S.T. & Ng, I.O. β-catenin mutation and overexpression in hepatocellular carcinoma: clinicopathologic and prognostic significance. *Cancer* **92**, 136–145 (2001).
15. Gunther, K. *et al.* Predictive value of nuclear β-catenin expression for the occurrence of distant metastases in rectal cancer. *Dis. Colon Rectum* **41**, 1256–1261 (1998).
16. Maruyama, K. *et al.* Cytoplasmic β-catenin accumulation as a predictor of hematogenous metastasis in human colorectal cancer. *Oncology* **59**, 302–309 (2000).
17. Hugh, T.J. *et al.* Beta-catenin expression in primary and metastatic colorectal carcinoma. *Int. J. Cancer* **82**, 504–511 (1999).
18. Chung, G.G. *et al.* Tissue microarray analysis of β-catenin in colorectal cancer shows nuclear phospho-β-catenin is associated with a better prognosis. *Clin. Cancer Res.* **7**, 4013–4020 (2001).
19. Lin, S.Y. *et al.* Nuclear localization of EGF receptor and its potential new role as a transcription factor. *Nature Cell Biol.* **3**, 802–808 (2001).

Automated subcellular localization and quantification of protein expression in tissue microarrays

ROBERT L. CAMP, GINA G. CHUNG & DAVID L. RIMM
Department of Pathology, Yale University School of Medicine, New Haven, Connecticut, USA
Correspondence should be addressed to D.L.R.; email: david.rimm@yale.edu

Published online 21 October 2002; doi:10.1038/nm791

Supplemental Material

Materials and methods

Tissue microarray design and processing. Paraffin-embedded, formalin-fixed specimens from 345 cases of node-positive breast carcinoma (1962–1977) and 310 cases of colon carcinoma (1971–1982) were obtained, as available, from the archives of the Yale University, Department of Pathology. Areas of invasive carcinoma, away from *in situ* lesions and normal epithelium, were identified and two 0.6-mm cores were taken from separate areas. Each core was arrayed into recipient blocks in a 1mm-spaced grid covering approximately 1 square inch, and 5-micron thick sections were cut and processed as previously described[1].

Immunohistochemistry. In brief, pre-cut paraffin-coated tissue microarray slides were deparaffinized and antigen-retrieved by pressure-cooking[2]. Slides were preincubated with 0.3% bovine serum albumin in 0.1M tris-buffered saline (pH 8.0) (BSA/TBS) for 30 min at room temperature. Slides were then incubated with primary antibodies diluted in BSA/TBS either for 1 h at room temperature or overnight at 4 °C. Slides were washed 3x 5 min with BSA/TBS containing 0.05% Tween-20. Corresponding secondary antibodies were applied for 1 h at room temperature in BSA/TBS. These included either antibodies directly conjugated to a fluorphore (Amersham, Piscataway, New Jersey and Molecular Probes, Eugene, Oregon), and/or conjugated to a horseradish peroxidase (HRP) decorated dextran-polymer backbone (Envision, DAKO, Carpinteria, California). DAPI was included with the secondary antibodies to visualize nuclei. Slides were again washed 3x 5 min with BSA/TBS containing 0.05% Tween-20. For manual analysis, slides were then incubated with diaminobenzidine (DAB, DAKO). For automated analysis, slides were incubated with a fluorescent chromagen (Cy-5-tyramide, NEN Life Science Products, Boston, Massachusetts) which, like DAB, is activated by HRP and results in the deposition of numerous covalently associated Cy-5 dyes immediately adjacent to the HRP-conjugated secondary antibody. Cy-5 (red) was used because its emission peak is well outside the green-orange spectrum of tissue autofluorescence. Slides for automated analysis were coverslipped with an antifade-containing mounting medium (Gelvatol with 0.6% n-propyl gallate). Manual examination of microarrays for ER and β-catenin levels has been previously described[3].

Specifically, four sets of primaries and secondaries were used:
Estrogen receptor (manual analysis): Primary: mouse monoclonal anti-ER (1:1 of clinical pre-diluted antibody, DAKO) for 1 h. Secondary: Envision anti-mouse for 1 h. Chromagen for Envision antibody: diaminobenzidine. Counterstain: ammonium hydroxide acidified hematoxylin.
Estrogen Receptor (automated analysis): Primary: mouse monoclonal anti-ER (1:1 of clinical pre-diluted antibody, DAKO) for 1 h and polyclonal rabbit anti-cytokeratin (1:50, Zymed, South San Francisco, California) for 1 h as a cocktail. Secondaries: Alexa 488-conjugated goat anti-rabbit (1:200, Molecular Probes, Eugene, Oregon), Envision anti-mouse (neat) and DAPI for 1 h as a cocktail. Chromagen for Envision antibody: Cy-5 tyramide.
Beta-catenin (manual analysis): Primaries: monoclonal anti-β-catenin (mouse clone 14, BD Transduction Labs, San Diego California). Secondary: Envision anti-mouse for 1 h. Chromagen for Envision antibody: diaminobenzidine. Counterstain: ammonium hydroxide acidified hematoxylin.
Beta-catenin (automated analysis): Primaries: monoclonal anti-β-catenin (mouse clone 14, BD Transduction Labs) and polyclonal rabbit anti-α-catenin for 1 h. Secondaries: Alexa 488-conjugated goat anti-rabbit, Envision anti-mouse and DAPI for 1 h. Chromagen for Envision antibody: Cy-5 tyramide.

Image acquisition. Images of microarrays were obtained using a Deltavision platform and software (SoftWorx 2.5; Applied Precision, Issaquah, Washington), with an attached water-cooled Photometrics series 300 camera through a x10 Nikon Super-Fluor lens on a TE200 inverted fluorescent microscope with automated *x*, *y*, *z* stage movement. Low power images of microarrays were stitched together using multiple (~1500) low-resolution images of the microarray (64 x 64 pixel) at approximately 7-micron resolution. Histospots were identified using signal from DAPI, cytokeratin, or α-catenin tags. This signal was thresholded to create a binary image of the microarray. Histospots were identified using size criteria. Rows and columns of histospots were then identified, and missing histospots filled in, allowing each histospot to be identified based on its row/column grid position. The coordinates of each histospot were then recorded. Subsequently, monochromatic, high-resolution (1024 x 1024 pixel, 0.5-micron resolution) images were obtained of each histospot, both in the plane of focus and 8 microns below it, and recorded in an image stack as bitmaps. This depth, slightly below the bottom of the tissue, was determined to be optimal for 5-micron histologic sections. A resolution of 0.5 microns is suitable for distinguishing between large subcellular compartments such as the cell membrane and nuclei. In theory, smaller compartments (for example, mitochondria, nucleoli) might require higher resolution. Images were obtained using a dynamic range of 0–1024, but saved and analyzed as 8-bit tiff images with a dynamic range of 0–255.

RESA/PLACE algorithmic analysis of images. First, a tumor-specific mask is generated by thresholding the image of a marker that differentiates tumor from surrounding stroma and/or leukocytes. This creates a binary mask (each pixel is either 'on' or 'off'). In this study we used cytokeratin and α-catenin to create tumor masks. As formalin-fixed tissues can exhibit autofluorescence, analysis may give multiple background peaks. The RESA/PLACE algorithms determine which of these peaks is predominant and sets a binary mask threshold at a slightly higher intensity level. This provides an adaptive (unique to each histospot) thresholding system that ensures that only the target signal from the tumor and not the surrounding elements is analyzed. Thresholding levels were verified by spot-checking a few images and then automated for the remaining images. This binary mask can be modified using standard image manipulations. In most cases this involves filling holes of a particular size (for example, less than 500 pixels, to fill in tumor nuclei that do not stain for either cytokeratin or α-catenin) and removing extraneous single pixels. Once set, these image manipulations are performed automatically on all images. All subsequent image manipulations involve only image information from the masked area.

Next, two images (one in-focus, one slightly deeper) are taken of the compartment-specific tags and the target marker. A percent-

age of the out-of-focus image is subtracted from the in-focus image, based on a pixel-by-pixel analysis of the two images. This percentage is determined according to the ratio of the highest/lowest intensity pixels in the in-focus image – representing the signal-to-noise ratio of the image. By using an exponential scale, this allows RESA to subtract low intensity pixels in images with a low signal-to-noise ratio less heavily than low intensity pixels from images with a high signal-to-noise ratio. The overall degree of subtraction is based on a user-defined percentage for each subcellular compartment. For most applications this is empirically set to 40% of the total signal, and remains constant for images from an entire microarray. RESA thus eliminates all out-of-focus information. The algorithm has the added benefit of enhancing the interface between areas of higher intensity staining and adjacent areas of lower intensity staining, allowing more accurate assignment of pixels of adjacent compartments. In contrast to the compartment-specific tags, the RESA subtraction of the target signal is uniform and not based on overall intensity of the image intensity. This ensures that the same amount of subtraction occurs with the target signal from all specimens.

Finally, the PLACE algorithm assigns each pixel in the image to a specific subcellular compartment (Supplemental Figs. 1 and 2). Pixels that cannot be accurately assigned to a compartment to within a user-defined degree of confidence (usually 95%) are discarded. This is accomplished iteratively by determining the ratio of signal from two compartment-specific markers that minimizes the spillover of marker from one compartment into another. Pixels where the nuclear and membrane pixel intensities are too similar to be accurately assigned are negated (usually comprising <8% of the total pixels). A third compartment (the cytoplasm) can be defined by exclusion (non-membrane, non-nuclear). Once each pixel is assigned to a subcellular compartment (or excluded as described above), the signal in each location is added up. This data is saved and can subsequently be expressed either as a percentage of total signal or as the average signal intensity per compartment area. The score is expressed on a scale of 1 to 1000 as the total intensity detectable in a pixel ranges from 1–255 creating 3 significant figures. These algorithms are described in a recently submitted patent of this technology owned by Yale University. In this study, for ER, only nuclear-localized signal was used; for β-catenin total signal, the ratio of nuclear to membrane signal, and the ratio of nuclear to total signal was analyzed. Scores were adjusted according to amount of area covered by the subcellular compartments within the masked area

Data analysis. Staining scores from the breast cancer histospots represent the averaged results from two independently scored histospots. Histospot containing <10% tumor, as assessed either subjectively (manual) or by mask area (automated), were excluded from further analysis. For the purposes of validation, we did not manually exclude any images of histospots exhibiting aberrant staining (for example, with normal epithelium or in situ carcinoma), although such manual assessment could be performed. Our previous studies have demonstrated that scores from the average of two histospots matches the score from an entire tissue section >95% of the time[4]. Subsequent studies revealed that analysis of a single histospot could provide significant statistical power to judge outcomes (data not shown), so that staining scores from the colon cancer array represent the result of only one histospot. Estrogen receptor expression showed continuous prognostic significance such that virtually any division between low and high expressers resulted in a significant survival difference; therefore, we chose the top and bottom 25th percentiles as arbitrary divisions for high and low expression. Overall survival analysis was assessed using Kaplan-Meier analysis and the Mantel-Cox log-rank score for assessing statistical significance. Relative risk was assessed using the univariate and multivariate Cox-proportional hazards model (Tables 1–4). Analyses were performed using Statview 5.0.1 (SAS Institute, Cary, North Carolina).

1. Kononen, J. *et al.* Tissue microarrays for high-throughput molecular profiling of tumor specimens. *Nature Med.* **4**, 844–847 (1998).
2. Katoh, A.K., Stemmler, N., Specht, S. & D'Amico, F. Immunoperoxidase staining for estrogen and progesterone receptors in archival formalin fixed, paraffin embedded breast carcinomas after microwave antigen retrieval. *Biotech. Histochem.* **72**, 291–298 (1997).
3. Snead, D.R. *et al.* Methodology of immunohistological detection of oestrogen receptor in human breast carcinoma in formalin-fixed, paraffin-embedded tissue: a comparison with frozen section methodology. *Histopathology* **23**, 233–238 (1993).
4. Camp, R.L., Charette, L.A. & Rimm, D.L. Validation of tissue microarray technology in breast carcinoma. *Lab. Invest.* **80**, 1943–1949 (2000).

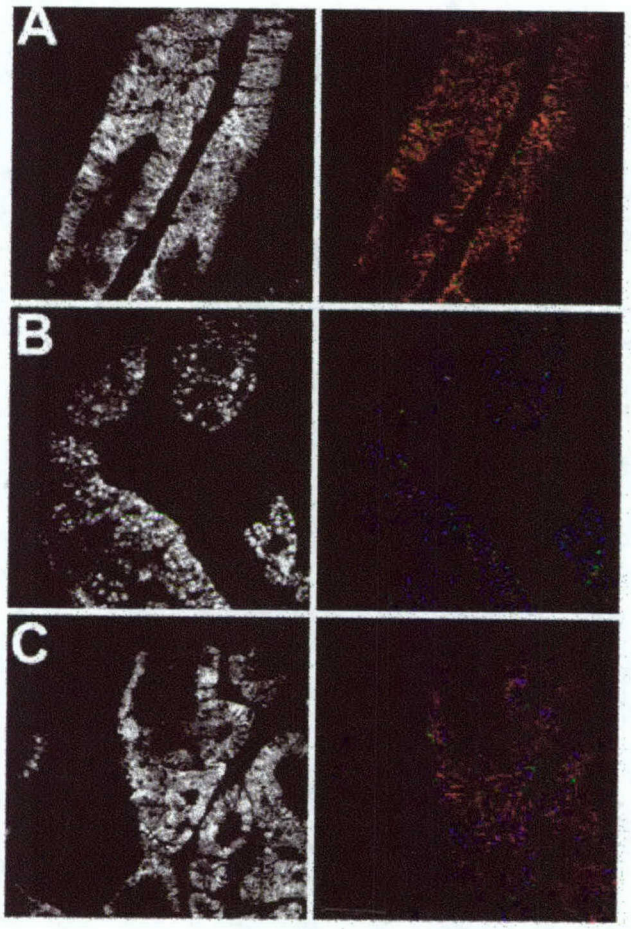

Fig. 1 Subcellular localization of β-catenin in three sample colon carcinomas. The importance of subcellular localization in automated analysis is exemplified by three colon carcinomas. An image of the carcinomas stained for β-catenin is shown of the left (grayscale), and the corresponding co-localization of that signal to subcellular compartments using RESA and PLACE is shown on the right (color). ***a***, Automated analysis of a colon carcinoma with predominantly membrane-associated β-catenin shows co-localization of the signal to the membrane (red) with little signal in the cytoplasm (green) or nuclei (blue). ***b***, Automated analysis of a carcinoma with predominantly nuclear-associated β-catenin shows co-localization of the signal to the nuclei (blue). ***c***, Automated analysis of a carcinoma with mixed β-catenin expression shows co-localization to both membrane (red), cytoplasmic (green) and nuclear (blue) compartments. Note that without subcellular localization, the overall expression of β-catenin in these three tumors would be similar. An additional confounding factor — the amount of surrounding desmoplastic stroma — is eliminated by using a mask (cytokeratin) that recognizes only tumor.

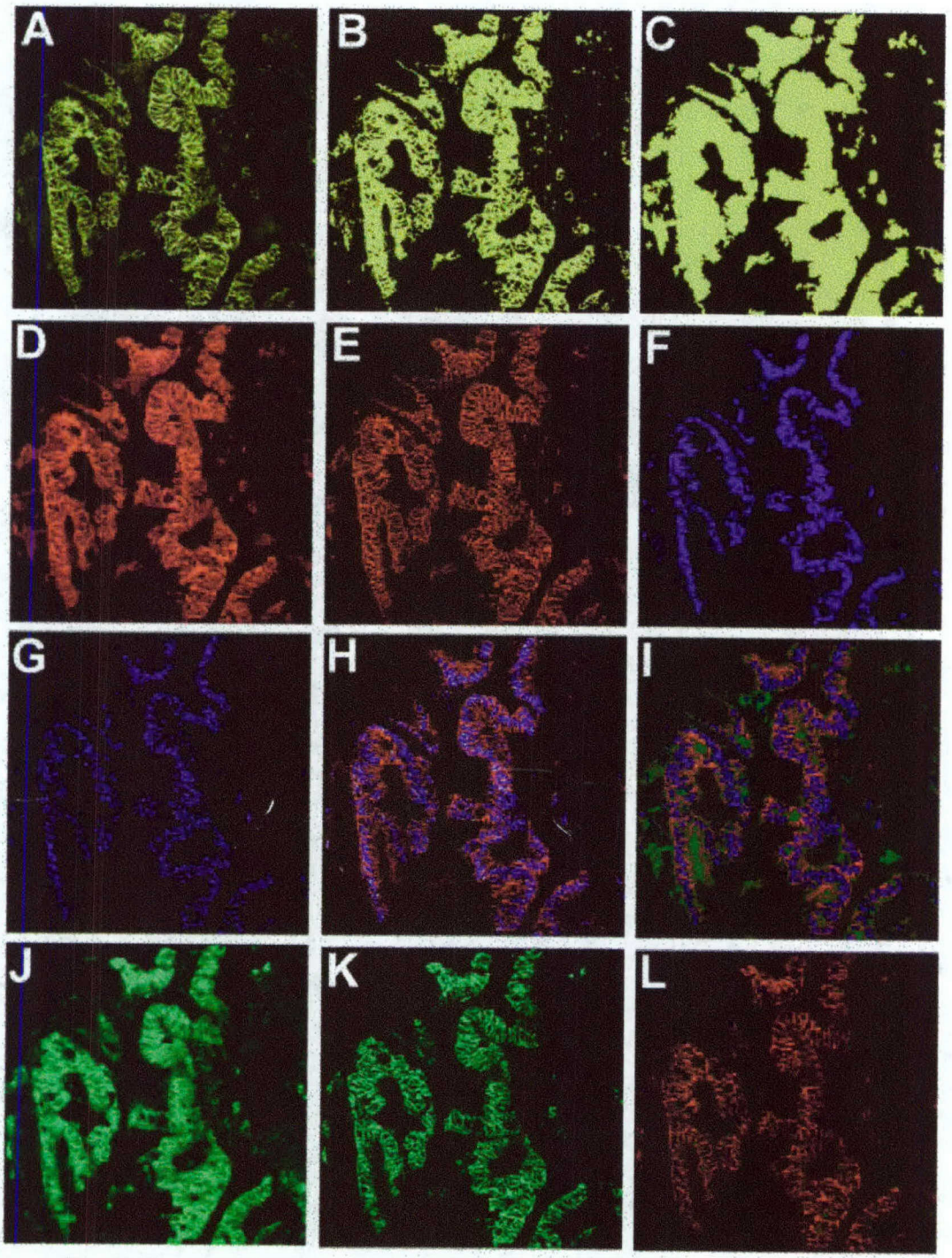

Fig. 2 Step-by-step methodology for RESA and PLACE algorithms. ***a***, Tumor cells are differentiated from stroma using a tumor-specific tag. Anti-cytokeratin is used to distinguish colon carcinoma from surrounding desmoplastic stroma. ***b***, The cytokeratin image is gated to form a binary mask. ***c***, The binary mask is enhanced by filling holes and removing small objects. ***d***, An image of the membrane-specific tag is taken. Anti-α-

catenin is used to tag the membrane of a colon carcinoma. ***e***, The membrane tag image is exponentially subtracted using RESA (Rapid Exponential Subtraction Algorithm). ***f***, An image of the nucleus-specific tag is taken. DAPI is used to tag the nuclei of a colon carcinoma. ***g***, The nuclear tag image is exponentially subtracted using RESA. ***h***, The membrane and nuclear tag images are merged, and overlapping pixels are identified and removed. White pixels represent overlap. ***i***, The membrane and nuclear compartments are overlaid on the tumor-specific mask. The overlay ensures that non-tumor nuclei and stroma are not included in the analysis of the target marker. ***j***, An image of the target-specific marker is taken, in this case, β-catenin expression of a colon carcinoma. ***k***, The target marker image is exponentially subtracted using RESA. ***l***, The intensity of the marker is divided into the various subcellular compartments. In this tumor, β-catenin is predominantly localized to the membrane (red) with minor amounts found in the nuclei (blue) and cytoplasm (green).

Table 1 Five-year multivariate analysis of survival

Variable	Relative Risk (95% C.I.)	*P*-value
Histologic Grade 3/3	1.100 (0.655–1.846)	0.7195
Nuclear Grade 3/3	1.096 (0.655–1.834)	0.7283
Age ³ 50 yrs	1.501 (0.791–2.850)	0.2140
Stage ³ iiia	**1.775 (1.051–2.998)**	**0.0318**
Low ER*	**2.566 (1.428–4.611)**	**0.0016**

Variables in boldface are statistically significant. *: Tumors with estrogen receptor (ER) levels in the bottom 25% were compared to tumors in the top 25%.

Table 2 Multivariate analysis of total nuclear and nuclear/membrane β-catenin ratios

	Total nuclear β-catenin*		Nuclear/membrane β-catenin†	
Variable	relative risk	*P*-value	relative risk	*P*-value
High β-catenin	1.118 (0.599–2.084)	0.7266	**1.865 (1.068–3.259)**	**0.0285**
TNM stage ³ T3	1.462 (0.926–2.309)	0.1033	1.527 (0.872–2.673)	0.1386
Nodal metastases	1.466 (0.963–2.227)	0.0739	1.490 (0.866–2.564)	0.1495
Poorly-differentiated	1.216 (0.624–2.032)	0.6929	1.490 (0.712–3.115)	0.2902
Age ³ 62-year old	**1.944 (1.162–3.252)**	**0.0113**	**2.412 (1.212–4.800)**	**0.0121**

Variables in boldface are statistically significant. *: Tumors with nuclear β-catenin levels in the top 10% were compared to the rest; †: tumors with nuclear/membrane β-catenin ratios in the top 25% were compared to the bottom 25%.

Table 3 Chi-square analysis of total nuclear and nuclear/membrane β-catenin ratios

	Total nuclear*	Nuclear/membrane ratio†
	P-value	*P*-value
TNM stage ³ T3	0.1622	0.7744
Presence of nodal metastases	**0.0136‡**	0.3979
Poorly-differentiated tumors	0.1392	0.9717
Age ³ 62-year old	0.8521	0.3459

Variables in boldface are statistically significant. *: Tumors with nuclear β-catenin levels in the top 10% were compared to the rest; †: tumors with nuclear/membrane β-catenin ratios in the top 25% were compared to the bottom 25%; ‡: 70% of tumors with high nuclear β-catenin were node-positive versus 41% of tumors with lower levels.

Table 4 Partial list of markers successfully analyzed using the RESA and PLACE algorithms

Marker	Source	Dilution	Predominant pattern(s)
EGFR	CST	1:50	nuclear, membrane
Phospho-EGFR (Y1068)	CST	1:50	nuclear, membrane
Phospho-EGFR (Y1045)	CST	1:50	membrane, cytoplasmic
Phospho-EGFR (Y845)	CST	1:50	nuclear, membrane
Phospho-EGFR (Y992)	CST	1:50	membrane, cytoplasmic
HER2/neu	DAKO	neat	membrane, cytoplasmic
Phospho-ERK (T202/Y204)	CST	1:100	nuclear, cytoplasmic
STAT3	CST	1:100	nuclear, cytoplasmic
Phospho-STAT3 (Y705)	CST	1:50	nuclear, cytoplasmic
KI-67	Trans.	1:250	nuclear
Na/K ATPase α1	Upstate	1:100	membrane
Laminin-beta 1	Upstate	1:100	peri-membranous
Heparan Sulfate	Seikagaku	1:50	peri-membranous
Alpha-catenin	BD	1:500	membrane
Beta-cateinin	BD	1:500	membrane, nucleus
Plakoglobin	BD	1:500	membrane
Cytokeratin AE1/AE3	DAKO	1:250	cytoplasmic
Cytokeratin polyclonal	Zymed	1:50	cytoplasmic
Spectrin	Yal e	1:50	membrane, cytoplasmic, nuclear
Survivin	Yale	1:100	cytoplasmic
CD44	BD	1:200	membrane

BD: BD Biosciences/Transduction Labs (San Diego, California); CST: Cell Signaling Technology (Beverly, Massachusetts); DAKO Corp (Carpenteria, California); Seikagaku America (Falmouth, Massachusetts); Upstate Biotech (Lake Placid, New York); Zymed (South San Francisco, California).

[CANCER RESEARCH 63, 1101–1105, March 1, 2003]

Appendix 2

Tissue Microarray Analysis of Hepatocyte Growth Factor/Met Pathway Components Reveals a Role for Met, Matriptase, and Hepatocyte Growth Factor Activator Inhibitor 1 in the Progression of Node-negative Breast Cancer[1]

Jung Y. Kang, Marisa Dolled-Filhart, Idris Tolgay Ocal, Baljit Singh, Chen-Yong Lin, Robert B. Dickson, David L. Rimm, and Robert L. Camp[2]

Department of Pathology, Yale University School of Medicine, New Haven, Connecticut 06520 [J. Y. K., M. D-F., I. T. O., D. L. R., R. L. C.], and Lombardi Cancer Center, Departments of Oncology and Pathology, Georgetown University School of Medicine, Washington, DC 20007 [B. S., C-Y. L., R. B. D.]

ABSTRACT

Numerous studies have demonstrated that overexpression of Met, the hepatocyte growth factor (HGF) receptor, plays an important role in tumorigenesis. Met activation can either occur through ligand-independent or -dependent mechanisms, both of which are mediated by a series of proteases and modulators. We studied the protein expression of several components of the HGF/Met pathway on a cohort of 330 node-negative breast carcinomas using a tissue microarray annotated with 30-year, disease-specific patient follow-up data. We examined HGF, matriptase (an activator of HGF expressed on mammary epithelial cell surfaces), HAI-I (the cognate inhibitor of matriptase), and the Met receptor itself. Our studies demonstrate tight correlation between the expression of HGF, matriptase, and Met in breast carcinoma. High-level expression of Met, matriptase, and HAI-I were associated with poor patient outcome. Met and HAI-I showed independent prognostic value when compared with traditional breast markers in a multivariate analysis. Intriguingly, antibodies against the intracellular but not the extracellular domain of Met were prognostic, suggesting that overexpression of the cytoplasmic-tail of Met, perhaps through cleavage or truncating mutation, may play an important role in breast cancer progression.

INTRODUCTION

Many studies have demonstrated the importance of the HGF[3] pathway in carcinogenesis (1). HGF is produced both by tumor cells as well as by surrounding stromal elements, and can act in either a paracrine or autocrine fashion (2–5). HGF is secreted as an inactive propeptide, which must be cleaved to become biologically active. One enzyme responsible for this cleavage is matriptase, an epithelial-localized transmembrane serine protease (6–8). Matriptase is, in turn, regulated by a naturally occurring inhibitor, HAI-1 (9, 10). When cleaved, HGF can bind to its receptor, Met, thereby stimulating multiple downstream pathways, leading to mitogenesis, motogenesis, and morphogenesis (11).

Several studies have analyzed individual components of the HGF pathway for their association with tumor aggression and/or patient survival. Early biochemical studies demonstrated that overall levels of HGF in breast cancers correlated with worse patient outcome (2, 3, 5). Whether HGF production by tumors and/or surrounding stroma is an important prognostic feature is unclear; although tumor cells themselves are a major producer of HGF (4, 5, 12). The use of matriptase and HAI-1 as prognostic markers in breast cancer has not been reported previously. However, recently, one study demonstrated that high matriptase and low HAI-1 levels were associated with advanced-stage ovarian tumors (13). Another report demonstrated that the glycosylation of matriptase stabilized and enhanced its proteolytic activity, and promoted tumor aggression (14).

The expression of Met has been more extensively studied. Met overexpression associates with poor prognosis in a variety of tumors (1). Whether such expression is ligand- (HGF) dependent or independent is unclear; however, the constitutive activation of Met, via several ligand-independent mechanisms, is established. These mechanisms include activating point mutations (15–19), chromosomal translocations (20, 21), and truncations of the cytoplasmic domain (22, 23). In addition, dysregulation of Met-associated phosphatases may also lead to Met activation (24).

We have now studied several elements of the HGF pathway including HGF, matriptase, HAI-1, and Met in a single cohort of node-negative breast cancer patients with 30-year follow-up, correlating the expression of each element and determining their prognostic value. This study was facilitated by the use of tissue microarrays: arrays of hundreds of patient histological samples on a single glass slide. Our study demonstrates a significant correlation between members of the HGF pathway and shows that several members have independent prognostic value in determining patient outcome.

MATERIALS AND METHODS

Cohort Design and Tissue Microarray Construction. Tissue microarrays were constructed, as described previously, and reviewed recently (25, 26). Three hundred and thirty cases of formalin-fixed, paraffin-embedded, node-negative breast carcinoma were obtained from the archives of the Department of Pathology, Yale University. Cases were taken sequentially, as available, from 1962 to 1980, with a median survival time of 15.6 years. Complete treatment history is not available from this cohort, but the vast majority of patients in this era were not treated with chemotherapy. Representative tumor regions were selected for coring by a pathologist (R. L. C.). Because prior studies have demonstrated that a single core adequately represents the staining pattern of an entire slide, all of the studies were performed using a single sample of each tumor (27, 28). Our previous study has also demonstrated the durability of antigens from archival specimens as old as 70 years (27). In the present study, all of the tumors demonstrated some degree of staining with one or more of the antibodies tested, demonstrating that no cases were antigenically "dead" because of fixation artifacts or tissue age.

Immunohistochemistry. Briefly, 5-μm tissue microarray slides were deparaffinized with xylene and ethanol. Antigen retrieval was performed using citrate buffer (pH 6.0) pressure-cooking (29). Primary antibodies were incubated overnight at 4°C, with the exception of antibodies to ERs, PRs, and Her2, which were incubated at room temperature for 1 h. Monoclonal anti-matriptase

Received 8/28/02; accepted 1/3/03.

The costs of publication of this article were defrayed in part by the payment of page charges. This article must therefore be hereby marked *advertisement* in accordance with 18 U.S.C. Section 1734 solely to indicate this fact.

[1] Supported by grants from the Patrick and Catherine Weldon Donaghue Foundation for Medical Research, The Connecticut Breast Cancer Alliance, and grants from the NIH, including National Institute of Environmental Health Sciences Grant K0-8 ES11571 (to R. L. C.), National Cancer Institute Grant RO-1 GM57604 (to D. L. R.), United States Army Grant DAMD 01-000436, and NIH Breast Cancer Specialized Programs of Research Excellence 2P50CA72460.

[2] To whom requests for reprints should be addressed, at Department of Pathology, Yale University, School of Medicine, 310 Cedar Street, BML 122, New Haven, CT 06520. E-mail: robert.camp@yale.edu.

[3] The abbreviations used are: HGF, hepatocyte growth factor; HAI, hepatocyte growth factor activator inhibitor; ER, estrogen receptor; PR, progesterone receptor; CI, confidence interval; uPA, urokinase-type plasminogen activator; PAI, plasminogen activator inhibitor.

and anti-HAI-1 antibodies were prepared as described previously (9, 30). Commercially acquired antibodies included: polyclonal (goat) anti-HGF antibody (R&D Systems, Minneapolis, MN); monoclonal antibody to the extracellular domain of Met (DO-24; Upstate Biotechnology, Lake Placid, NY); and monoclonal antibody to the intracellular domain of Met (3D4; Zymed, South San Francisco, CA). The specificities of all of the antibodies used were verified using immunoprecipitation and Western blotting. Antibodies to ER, PR, and HER-2/*neu* were obtained from DAKO (Carpinteria, CA) and used according to the manufacturer's specifications. Antibodies were either detected using a Vectastain ABC kit (Vector Laboratories, Burlingame, CA) for anti-HAI-1 or the DAKO Envision TM + System (DAKO) for the others. Signal from the HGF antibody was amplified using biotin-tyramide signal amplification followed by a streptavidin-horseradish peroxidase conjugate (TSA kit; Perkin-Elmer Life Sciences, Boston, MA). Staining was visualized using diaminobenzidine and counterstained with acidified hematoxylin. Slides were also stained in the absence of primary antibody to evaluate nonspecific secondary antibody reactions.

Evaluation of Immunostaining. Immunostaining was scored on a scale of 0 to 3+ (negative/weak/moderate/intense staining). Distinctions between membrane and cytoplasmic staining were impractical given the diffuse staining of the antigens (visualized using the chromogenic substrate, diaminobenzidine). Therefore, scores represent the combined staining intensity of membranous and cytoplasmic staining. Histospots with <10% of their area covered by tumor were excluded from analysis. Scoring was performed by two independent observers (J. Y. K. and M. D-F.), and histocores with discrepant scores were re-examined by both observers to achieve a consensus score. Cases with scores of 2+ or 3+ were designated as "high," whereas cases with scores of 0 or 1+ were designated as "low."

Statistical Analysis. All of the analyses were completed using Statview 5.0.1 (SAS Institute Inc., Cary, NC). Correlations between markers were performed using a χ^2 test. Prognostic significance was assessed using both univariate and multivariate Cox proportional hazards models with 30-year survival as an end point. Survival curves were calculated using the Kaplan-Meier method, with significance evaluated using the Manel-Cox log rank test.

RESULTS

We analyzed the expression of several components of the Met pathway including HGF, matriptase, HAI-1, and Met itself (using both intracellular- and extracellular-specific antibodies; Fig. 1). The number of tumors expressing high levels of these antigens ranged from 18 to 46% (Table 1). Although tissue microarrays have been shown to adequately represent tumor antigen expression (27), they most likely do not fully represent the expression of stromal markers. Therefore, we limited our analysis to the expression of markers by tumor cells and not stroma. In the case of HGF, this resulted in our selective study of autocrine (tumor) expression.

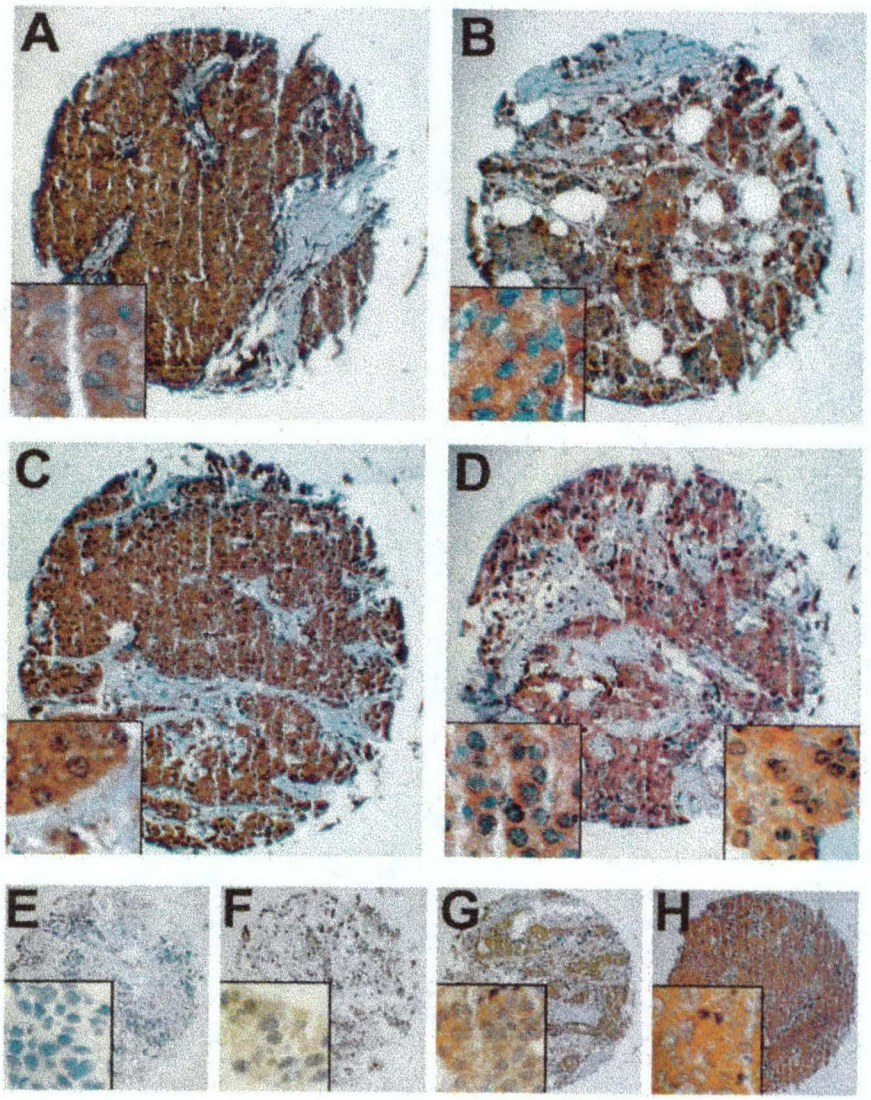

Fig. 1. Immunohistochemical staining of breast cancer tissue microarrays for four members of the HGF/Met pathway. Each histospot shows a representative positive case (3+) for matriptase (*A*), HAI-1 (*B*), HGF (*C*), and Met (*D*), at low (×40) and high (×200, *insets*) magnification. Matriptase, HAI-1, and Met show a membrano-cytoplasmic localization, whereas HGF is predominantly cytoplasmic. The cellular localization of Met using antibodies to the intracellular and extracellular domains was comparable (*D, left* and *right insets,* respectively). Representative histospots stained using an antibody to the intracellular domain of Met and scored as 0, 1, 2, or 3+ are shown in *E–H,* respectively.

Table 1 *Marker expression*[a]

Marker	Low (%)	High (%)	Total
Met (cytoplasmic)	229 (72)	91 (28)	320
Met (extracellular)	251 (78)	72 (22)	323
Matriptase	181 (55)	148 (45)	329
HGF	176 (54)	147 (46)	323
HAI-1	260 (82)	56 (18)	316
ER	212 (69)	95 (31)	307
PR	203 (68)	97 (32)	300
HER2/*neu*	260 (87)	38 (13)	298
Nuclear grade III	241 (81)	56 (19)	297
Patient age (>50 y)	225 (68)	105 (31)	330
Tumor size (>2 cm)	180 (45)	150 (55)	330

[a] The expression of experimental and traditional markers in a cohort of 330 node-negative breast cancer patients. Immunohistochemical stains were score on a four-point scale (0–3+), and divided into low (0–1+) and high (2+–3+) categories.

Table 2 *Met pathway associations: χ^2 analysis*[a]

	Met (cyto)	Met (extra)	Matriptase	HGF
Met (extra)	**<0.0001**			
Matripase	**<0.0001**	0.2588		
HGF	**0.0001**	**0.0002**	**<0.0001**	
HAI-I	0.3716	0.8320	0.0597	0.2902

[a] The association among expression of matriptase, HGF, HAI-1, and Met (using antibodies to both the cytoplasmic and extracellular domains) were determined using χ^2 analysis. Statistically significant observations are in boldface. All significant associations are direct (i.e. high-expression of one marker correlates with high-expression of the other).

Table 3 *Univariate analysis*[a]

Marker—high expression	*P*	Relative risk	95% CI
Met (cytoplasmic)	**0.0029**	1.826	1.228–2.715
Met (extracellular)	0.9771	1.007	0.639–1.585
Matriptase	**0.0279**	1.527	1.047–2.226
HGF	0.5026	1.140	0.778–1.670
HAI-1	**0.0110**	1.808	1.145–2.853
ER	0.3663	1.214	0.797–1.850
PR	0.7881	0.945	0.627–1.424
HER2/*neu*	0.4535	0.786	0.420–1.473
Nuclear grade III	0.7993	0.934	0.555–1.574
Patient age (>50 yr)	0.3240	1.227	0.817–1.843
Tumor size (>2 cm)	**0.0001**	2.134	1.448–3.145

[a] Univariate analysis of 30-year disease-related survival was performed using the Cox-proportional hazards model. Statistically significant observations are in boldface.

To elucidate potential associations between these markers, we performed χ^2 analyses, which revealed highly significant associations between the expression of Met, HGF, and matriptase ($P < 0.0002$; Table 2). HAI-1 expression was independent of these markers, although it trended toward coexpression with matriptase ($P = 0.0597$). Interestingly, the expression of antibodies to the intracellular and extracellular domains of Met were highly correlated ($P < 0.0001$; Table 2), but not coincident; 38 cases were scored as entirely Met-extracellular negative (score of 0) and Met-intracellular high (12.2%), whereas only 1 case was judged as entirely Met-intracellular negative and Met-extracellular high (0.3%). This result suggests that relative overexpression of the intracellular domain of Met is far more common than relative overexpression of the extracellular domain.

To determine the predictive power of the Met pathway, we initially performed a univariate analysis of individual Met pathway components and compared them with traditional breast cancer markers (Table 3). Because breast carcinoma can recur and kill patients decades after its initial diagnosis, we studied 30-year disease-related survival. Using univariate analysis, only the cytoplasmic tail of Met, not the extracellular portion, showed prognostic power ($P = 0.0029$; Table 3). Sixty-one percent of patients overexpressing the cytoplasmic domain of Met died of breast cancer within 30 years compared with 41% with lower levels. High-level matriptase expression was also predictive of poor outcome (51% dead of disease *versus* 40%; $P = 0.0279$; Table 3), as were elevated levels of HAI-1 (59% *versus* 40% survival; $P = 0.0110$; Table 3). Of the traditional markers of tumor aggression, only tumor size was predictive of outcome ($P = 0.0001$; Table 3). Kaplan-Meier curves demonstrated that these markers were prognostic over the entire 30-year follow-up period (Fig. 2).

Previous studies have suggested that the ratio of HAI-1 and matriptase may play an important role in promoting tumor aggression (13). Therefore, we compared the survival of patients with tumors expressing high and/or low levels of each. Among tumors expressing high levels of matriptase, HAI-1 coexpression predicted a worse outcome (relative risk = 1.88; 95% CI, 1.05–3.36; $P = 0.0335$). Comparison of tumors expressing both markers to those expressing neither demonstrated that patients with double-positive tumors have an increase relative risk of 2.43 (95% CI, 1.36–4.34; $P = 0.0026$). Addition of Met (cytoplasmic domain) to this analysis showed that patients with Met, matriptase, and HAI-1-positive tumors exhibit an increased relative risk of 3.25 (95% CI, 1.24–8.50; $P = 0.0165$).

We then determined the independent predictive power of the Met pathway. First, we limited our analysis solely to the Met pathway components. Using multivariate analysis, both the cytoplasmic tail of Met and HAI-1 retained independent predictive power (Table 4). When we included these two markers with traditional breast cancer markers, they retained their independence. Tumor size was the only other independent predictor of poor outcome (Table 5).

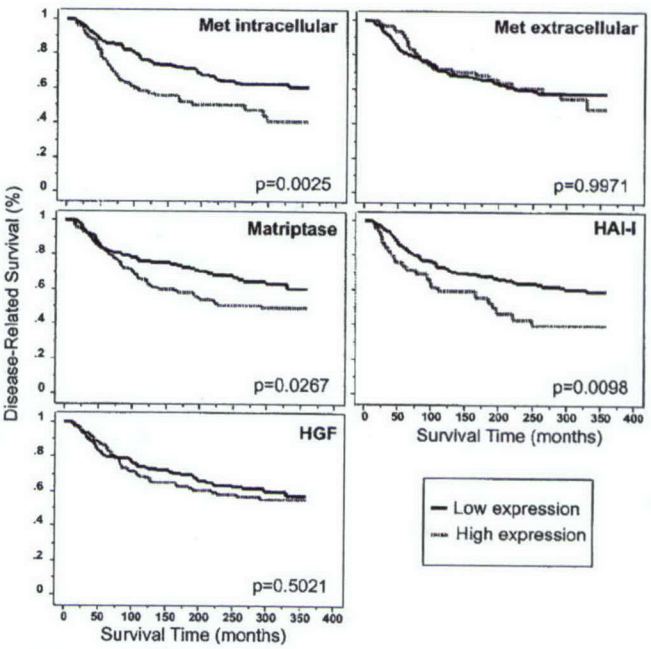

Fig. 2. Kaplan-Meier analysis of disease-related survival demonstrates that Met (intracellular domain), matriptase, and HAI-1 show long-term prognostic benefit. Statistical significance was assessed using the log rank test.

Table 4 *Multivariate analysis: Met pathway*[a]

Marker—high expression	*P*	Relative risk	95% CI
Met (cytoplasmic)	**0.0064**	1.862	1.191–2.910
Met (extracellular)	0.7710	1.079	0.645–1.805
Matriptase	0.2413	1.290	0.843–1.974
HGF	0.5189	1.159	0.740–1.815
HAI-1	**0.0291**	1.721	1.057–2.803

[a] Multivariate analysis of 30-year disease-related survival was performed using the Cox-proportional hazards model using only the experimental markers. Statistically significant observations are in boldface.

Table 5 *Multivariate analysis: traditional markers*[a]

Marker—high expression	*P*	Relative risk	95% CI
Met (cytoplasmic)	**0.0098**	1.841	1.159–2.925
HAI-1	**0.0483**	1.805	1.004–3.242
ER	0.8552	1.597	0.568–1.597
PR	0.9040	0.970	0.590–1.596
HER2/*neu*	0.5284	0.783	0.367–1.674
Nuclear grade III	0.7886	1.084	0.602–1.952
Patient age (>50 yr)	0.5320	1.177	0.706–1.963
Tumor size (>2 cm)	**0.0007**	2.265	1.415–3.627

[a] Multivariate analysis of 30-year disease-related survival was performed using the Cox-proportional hazards model using both the independent markers from Table 4 and traditional histopathologic measures. Statistically significant observations are in boldface.

DISCUSSION

The relative importance of ligand-dependent and ligand-independent Met activation in carcinogenesis is a matter of continued debate (1). Our studies demonstrate that members of the HGF pathway, namely HGF, Met, and matriptase, are often coexpressed on breast cancers, and that high-level expression of two of these members, Met and matriptase, associates with more aggressive tumors. Such observations would be expected if HGF-mediated Met stimulation played a role in tumorigenesis. Although tumoral HGF levels were not found to be predictive of outcome, the expression of matriptase was prognostic in a univariate analysis, suggesting that as an activator of HGF, it plays a rate-dependent ("gate-keeping") role in the ligand-dependent stimulation of Met.

In addition to their role in the activation of HGF, matriptase and its cognate inhibitor, HAI-1, also play a role in the plasminogen activator cascade (6, 31, 32). This cascade culminates in the activation of plasmin and the coactivation of matrix metalloproteinases, both of which degrade extracellular matrix components and potentiate tumor cell invasion, extravasation, and metastasis (33). Matriptase promotes this pathway by activating latent uPA, which, in turn, activates plasmin (6, 34). Like matriptase, uPA can also cleave pro-HGF, providing another level of interaction between the Met/HGF pathway and plasmin cascade (35). Given the multiple functions of matriptase, it is not surprising that aggressive breast tumors produce higher levels of this enzyme.

Likewise, HAI-1, as an inhibitor of matriptase, may help modulate both the Met/HGF and plasmin pathways. Interestingly, the expression of HAI-I was independent of the other members of the Met pathway indicating that its expression is regulated differently. Previous reports have suggested that HAI-I is down-regulated in colon carcinoma and high-grade ovarian carcinomas (13, 36). In contrast, our study demonstrates that HAI-1 expression is associated with aggressive breast carcinomas, being an independent predictor of poor outcome (Table 5). Although this may be puzzling in light of the role of HAI-1 in inhibiting HGF-dependent Met activation, the coordinated expression of both matriptase and HAI-1 may be far more important in promoting tumor aggression than the unopposed production of active matriptase in the absence of its inhibitor. Coordinated regulation of another inhibitor of the uPA/plasmin cascade, PAI-1, is crucial for inducing tumor invasion (37). Furthermore, a recent meta-analysis of the uPA/PAI-1 system in breast cancer demonstrated conclusively that overexpression of both uPA and its inhibitor PAI-1 were associated with poor outcome in breast cancer (32). In our study, the importance of matriptase and HAI-1 coexpression is demonstrated in the elevated relative risk of patients with tumor expressing both markers.

Because of lot-to-lot inconsistencies in polyclonal Met-antibodies,[4] we analyzed two different monoclonal antibodies, one to the extracellular and one to the intracellular domain. Comparison of Met expression as assessed by these two antibodies showed some interesting results. First, the expression of the intra- and extracellular domains of Met, although highly associated, was not coincident. Second, of cases with mixed expression of intra- and extracellular Met, overexpression of the intracellular domain was far more common, with 12.2% of all of the cases expressing solely the intracellular domain. Third, high levels of the cytoplasmic tail of Met were predictive of poor outcome, whereas expression of the extracellular portion was not. Although this result could be explained by differences in the affinity of the antibodies for Met in formalin-fixed, paraffin-embedded tissue, both antibodies gave strong staining and similar results across a range of titrations (data not shown). A more likely explanation is that the cytoplasmic tail of Met is either cleaved (*e.g.*, after activation) or that mutations in Met lead to an overexpression of the cytoplasmic tail in some tumors. Indeed, recent studies have suggested that the cleavage of the cytoplasmic tail of Met may be important in signal transduction (1, 22, 23). Whether overexpression of the Met intracellular domain relative to the extracellular domain is a ligand-independent or -dependent phenomenon is unclear. Interestingly, expression of the Met extracellular domain correlates with HGF levels but not matriptase levels, whereas the Met intracellular domain correlates with both. This observation would be expected if the binding of matriptase-potentiated HGF to Met induced a subsequent cleavage of the Met intracellular domain.

In summary, we have made use of tissue microarray technology to analyze various components of the Met-signaling pathway. Our studies provide evidence that the expression of the stimulatory members of this pathway (Met, HGF, and matriptase) is tightly correlated. High-level HAI-1 expression is an independent predictor of outcome. Furthermore, studies using antibodies to different domains of the Met receptor suggest that overexpression of the cytoplasmic domain is a strong independent predictor of outcome.

[4] Unpublished observations.

ACKNOWLEDGMENTS

We thank Thomas D'Aquila and Lori Charette for their help in this effort.

REFERENCES

1. Danilkovitch-Miagkova, A., and Zbar, B. Dysregulation of Met receptor tyrosine kinase activity in invasive tumors. J. Clin. Investig., *109:* 863–867, 2002.
2. Yao, Y., Jin, L., Fuchs, A., Joseph, A., Hastings, H. M., Goldberg, I. D., and Rosen, E. M. Scatter factor protein levels in human breast cancers: clinicopathological and biological correlations. Am. J. Pathol., *149:* 1707–1717, 1996.
3. Jin, L., Fuchs, A., Schnitt, S. J., Yao, Y., Joseph, A., Lamszus, K., Park, M., Goldberg, I. D., and Rosen, E. M. Expression of scatter factor and c-met receptor in benign and malignant breast tissue. Cancer (Phila.), *79:* 749–760, 1997.
4. Tsao, M. S., Yang, Y., Marcus, A., Liu, N., and Mou, L. Hepatocyte growth factor is predominantly expressed by the carcinoma cells in non-small-cell lung cancer. Hum. Pathol., *32:* 57–65, 2001.
5. Wang, Y., Selden, A. C., Morgan, N., Stamp, G. W., and Hodgson, H. J. Hepatocyte growth factor/scatter factor expression in human mammary epithelium. Am. J. Pathol., *144:* 675–682, 1994.
6. Lee, S. L., Dickson, R. B., and Lin, C. Y. Activation of hepatocyte growth factor and urokinase/plasminogen activator by matriptase, an epithelial membrane serine protease. J. Biol. Chem., *275:* 36720–36725, 2000.
7. Tanimoto, H., Underwood, L. J., Wang, Y., Shigemasa, K., Parmley, T. H., and O'Brien. T. J. Ovarian tumor cells express a transmembrane serine protease: a potential candidate for early diagnosis and therapeutic intervention. Tumor Biol., *22:* 104–114, 2001.
8. Oberst, M., Anders, J., Xie, B., Singh, B., Ossandon, M., Johnson, M., Dickson, R. B., and Lin, C. Y. Matriptase and HAI-1 are expressed by normal and malignant epithelial cells *in vitro* and *in vivo*. Am. J. Pathol., *158:* 1301–1311, 2001.
9. Lin, C. Y., Anders, J., Johnson, M., and Dickson, R. B. Purification and characterization of a complex containing matriptase and a Kunitz-type serine protease inhibitor from human milk. J. Biol. Chem., *274:* 18237–18242, 1999.
10. Shimomura, T., Denda, K., Kitamura, A., Kawaguchi, T., Kito, M., Kondo, J., Kagaya, S., Qin, L., Takata, H., Miyazawa, K., and Kitamura, N. Hepatocyte growth factor activator inhibitor, a novel Kunitz-type serine protease inhibitor. J. Biol. Chem., *272:* 6370–6376, 1997.

11. Boccaccio, C., Ando, M., Tamagnone, L., Bardelli, A., Michieli, P., Battistini, C., and Comoglio, P. M. Induction of epithelial tubules by growth factor HGF depends on the STAT pathway. Nature (Lond.), *391:* 285–288, 1998.
12. Edakuni, G., Sasatomi, E., Satoh, T., Tokunaga, O., and Miyazaki, K. Expression of the hepatocyte growth factor/c-Met pathway is increased at the cancer front in breast carcinoma. Pathol. Int., *51:* 172–178, 2001.
13. Oberst, M. D., Johnson, M. D., Dickson, R. B., Lin, C. Y., Singh, B., Stewart, M., Williams, A., al-Nafussi, A., Smyth, J. F., Gabra, H., and Sellar, G. C. Expression of the serine protease matriptase and its inhibitor HAI-1 in epithelial ovarian cancer: correlation with clinical outcome and tumor clinicopathological parameters. Clin. Cancer Res., *8:* 1101–1107, 2002.
14. Ihara, S., Miyoshi, E., Ko, J. H., Murata, K., Nakahara, S., Honke, K., Dickson, R. B., Lin, C. Y., and Taniguchi, N. Prometastatic effect of N-acetylglucosaminyltransferase V is due to modification and stabilization of active matriptase by adding β 1–6 GlcNAc branching. J. Biol. Chem., *277:* 16960–16967, 2002.
15. Park, W. S., Dong, S. M., Kim, S. Y., Na, E. Y., Shin, M. S., Pi, J. H., Kim, B. J., Bae, J. H., Hong, Y. K., Lee, K. S., Lee, S. H., Yoo, N. J., Jang, J. J., Pack, S., Zhuang, Z., Schmidt, L., Zbar, B., and Lee, J. Y. Somatic mutations in the kinase domain of the Met/hepatocyte growth factor receptor gene in childhood hepatocellular carcinomas. Cancer Res., *59:* 307–310, 1999.
16. Di Renzo, M. F., Olivero, M., Martone, T., Maffe, A., Maggiora, P., Stefani, A. D., Valente, G., Giordano, S., Cortesina, G., and Comoglio, P. M. Somatic mutations of the MET oncogene are selected during metastatic spread of human HNSC carcinomas. Oncogene, *19:* 1547–1555, 2000.
17. Moon, Y. W., Weil, R. J., Pack, S. D., Park, W. S., Pak, E., Pham, T., Karkera, J. D., Kim, H. K., Vortmeyer, A. O., Fuller, B. G., and Zhuang, Z. Missense mutation of the MET gene detected in human glioma. Mod. Pathol., *13:* 973–977, 2000.
18. Schmidt, L., Duh, F. M., Chen, F., Kishida, T., Glenn, G., Choyke, P., Scherer, S. W., Zhuang, Z., Lubensky, I., Dean, M., Allikmets, R., Chidambaram, A., Bergerheim, U. R., Feltis, J. T., Casadevall, C., Zamarron, A., Bernues, M., Richard, S., Lips, C. J., Walther, M. M., Tsui, L. C., Geil, L., Orcutt, M. L., Stackhouse, T., Zbar, B., and *et al.* Germline and somatic mutations in the tyrosine kinase domain of the MET proto-oncogene in papillary renal carcinomas. Nat. Genet., *16:* 68–73, 1997.
19. Lee, J. H., Han, S. U., Cho, H., Jennings, B., Gerrard, B., Dean, M., Schmidt, L., Zbar, B., and Vande Woude, G. F. A novel germ line juxtamembrane Met mutation in human gastric cancer. Oncogene, *19:* 4947–4953, 2000.
20. Cooper, C. S., Park, M., Blair, D. G., Tainsky, M. A., Huebner, K., Croce, C. M., and Vande Woude, G. F. Molecular cloning of a new transforming gene from a chemically transformed human cell line. Nature (Lond.), *311:* 29–33, 1984.
21. Rodrigues, G. A., and Park, M. Dimerization mediated through a leucine zipper activates the oncogenic potential of the met receptor tyrosine kinase. Mol. Cell. Biol., *13:* 6711–6722, 1993.
22. Zhen, Z., Giordano, S., Longati, P., Medico, E., Campiglio, M., and Comoglio, P. M. Structural and functional domains critical for constitutive activation of the HGF-receptor (Met). Oncogene, *9:* 1691–1697, 1994.
23. Wallenius, V., Hisaoka, M., Helou, K., Levan, G., Mandahl, N., Meis-Kindblom, J. M., Kindblom, L. G., and Jansson, J. O. Overexpression of the hepatocyte growth factor (HGF) receptor (Met) and presence of a truncated and activated intracellular HGF receptor fragment in locally aggressive/malignant human musculoskeletal tumors. Am. J. Pathol., *156:* 821–829, 2000.
24. Rusciano, D., Lorenzoni, P., and Burger, M. M. Constitutive activation of c-Met in liver metastatic B16 melanoma cells depends on both substrate adhesion and cell density and is regulated by a cytosolic tyrosine phosphatase activity. J. Biol. Chem., *271:* 20763–20769, 1996.
25. Rimm, D. L., Camp, R. L., Charette, L. A., Olsen, D. A., and Provost, E. Amplification of tissue by construction of tissue microarrays. Exp. Mol. Pathol., *70:* 255–264, 2001.
26. Kononen, J., Bubendorf, L., Kallioniemi, A., Barlund, M., Schraml, P., Leighton, S., Torhorst, J., Mihatsch, M. J., Sauter, G., and Kallioniemi, O. P. Tissue microarrays for high-throughput molecular profiling of tumor specimens. Nat. Med., *4:* 844–847, 1998.
27. Camp, R. L., Charette, L. A., and Rimm, D. L. Validation of tissue microarray technology in breast carcinoma. Lab. Investig., *80:* 1943–1949, 2000.
28. Torhorst, J., Bucher, C., Kononen, J., Haas, P., Zuber, M., Kochli, O. R., Mross, F., Dieterich, H., Moch, H., Mihatsch, M., Kallioniemi, O. P., and Sauter, G. Tissue microarrays for rapid linking of molecular changes to clinical endpoints. Am. J. Pathol., *159:* 2249–2256, 2001.
29. Norton, A. J., Jordan, S., and Yeomans, P. Brief, high-temperature heat denaturation (pressure cooking): a simple and effective method of antigen retrieval for routinely processed tissues. J. Pathol., *173:* 371–379, 1994.
30. Lin, C. Y., Wang, J. K., Torri, J., Dou, L., Sang, Q. A., and Dickson, R. B. Characterization of a novel, membrane-bound, 80-kDa matrix-degrading protease from human breast cancer cells. Monoclonal antibody production, isolation, and localization. J. Biol. Chem., *272:* 9147–9152, 1997.
31. Oberst, M., Lin, C. Y., Dickson, R. B., and Johnson, M. Role of Proteases in Breast Cancer. J. Women Cancer, *2:* 201–216, 2002.
32. Look, M. P., van Putten, W. L., Duffy, M. J., Harbeck, N., Christensen, I. J., Thomssen, C., Kates, R., Spyratos, F., Ferno, M., Eppenberger-Castori, S., Sweep, C. G., Ulm, K., Peyrat, J. P., Martin, P. M., Magdelenat, H., Brunner, N., Duggan, C., Lisboa, B. W., Bendahl, P. O., Quillien, V., Daver, A., Ricolleau, G., Meijer-van Gelder, M. E., Manders, P., Fiets, W. E., Blankenstein, M. A., Broet, P., Romain, S., Daxenbichler, G., Windbichler, G., Cufer, T., Borstnar, S., Kueng, W., Beex, L. V., Klijn, J. G., O'Higgins, N., Eppenberger, U., Janicke, F., Schmitt, M., and Foekens, J. A. Pooled analysis of prognostic impact of urokinase-type plasminogen activator and its inhibitor PAI-1 in 8377 breast cancer patients. J. Natl. Cancer Inst., *94:* 116–128, 2002.
33. Andreasen, P. A., Kjoller, L., Christensen, L., and Duffy, M. J. The urokinase-type plasminogen activator system in cancer metastasis: a review. Int. J. Cancer, *72:* 1–22, 1997.
34. Takeuchi, T., Harris, J. L., Huang, W., Yan, K. W., Coughlin, S. R., and Craik, C. S. Cellular localization of membrane-type serine protease 1 and identification of protease-activated receptor-2 and single-chain urokinase-type plasminogen activator as substrates. J. Biol. Chem., *275:* 26333–26342, 2000.
35. Mars, W. M., Zarnegar, R., and Michalopoulos, G. K. Activation of hepatocyte growth factor by the plasminogen activators uPA and tPA. Am. J. Pathol., *143:* 949–958, 1993.
36. Kataoka, H., Hamasuna, R., Itoh, H., Kitamura, N., and Koono, M. Activation of hepatocyte growth factor/scatter factor in colorectal carcinoma. Cancer Res., *60:* 6148–6159, 2000.
37. Bajou, K., Noel, A., Gerard, R. D., Masson, V., Brunner, N., Holst-Hansen, C., Skobe, M., Fusenig, N. E., Carmeliet, P., Collen, D., and Foidart, J. M. Absence of host plasminogen activator inhibitor 1 prevents cancer invasion and vascularization. Nat. Med., *4:* 923–928, 1998.

Tissue Microarray-Based Studies of Patients with Lymph Node Negative Breast Carcinoma Show that Met Expression Is Associated with Worse Outcome but Is Not Correlated with Epidermal Growth Factor Family Receptors

Idris Tolgay Ocal, M.D.
Marisa Dolled-Filhart, B.S.
Thomas G. D'Aquila, B.S.
Robert L. Camp, M.D., Ph.D.
David L. Rimm, M.D., Ph.D.

Department of Pathology, Yale University School of Medicine, New Haven, Connecticut.

Supported by grants to David L. Rimm from the Patrick and Catherine Weldon Donaghue Foundation for Medical Research, the United States Army Breast Cancer Research Program (grant DAMD-17-01-0463) and the National Institutes of Health.

This article is dedicated to Joan D'Aquila.

Address for reprints: David L. Rimm, M.D., Ph.D., Department of Pathology, Yale University School of Medicine, 310 Cedar Street, New Haven, CT 06510; Fax: (203) 737-5089; E-mail: david.rimm@yale.edu

Received July 31, 2002; revision received January 3, 2003; accepted January 7, 2003.

BACKGROUND. It has been shown that receptor tyrosine kinases (RTKs) predict outcome in patients with breast carcinoma. Although RTKs are a large family, HER-2, epidermal growth factor receptor (EGFR), Met (hepatocyte growth factor receptor), and others all have shown the ability to predict outcome. However, it remains unclear whether these markers are defining the same subpopulation of patients with breast carcinoma. In this study, the authors attempted to determine the correlation between RTKs on the basis of their ability to stratify a population according to outcome.

METHODS. The authors used tissue microarray technology to study 324 patients with lymph node negative breast carcinoma who had 20–40 years of follow-up. Expression was assessed using immunohistochemical stains for Met, EFGR, fibroblast growth factor receptor (FGFR), and HER-2. Expression levels were assessed by two observers, and correlations were analyzed. Standard pathology information, including tumor size, nuclear grade, Ki-67 receptor status, and estrogen and progesterone receptor expression levels, also was collected.

RESULTS. RTK expression in the study cohort revealed two strong correlations. Specifically, HER-2 and EGFR showed similar expression patterns ($P < 0.0001$), and Met cytoplasmic domain and FGFR cytoplasmic staining showed similar expression patterns ($P < 0.0001$), but no correlation was found between the two groups. Of these RTKs, only high levels of Met cytoplasmic domain showed significance as a prognostic marker defining a shortened survival compared with the rest of the population ($P = 0.0035$; relative risk, 2.04). In the same group of patients, HER-2, hormone receptor status, and other RTK family receptors were not correlated with outcome. In multivariate analysis, only Met cytoplasmic domain and tumor size showed independent predictive value.

CONCLUSIONS. The current results indicate that the cytoplasmic domain of Met shows a unique staining pattern and defines a set of patients unique from the set of patients defined by overexpression of HER-2, EGFR, or hormone receptors. Furthermore, this group of patients is associated tightly and independently with worse outcome. ***Cancer* 2003;97:1841–8.** *© 2003 American Cancer Society.*
DOI 10.1002/cncr.11335

KEYWORDS: hepatocyte growth factor, c-met, adhesion, scatter factor, prognostic, ErbB2.

The single best indicator of disease free survival and overall survival in patients with breast carcinoma is lymph node status.[1] Patients who have breast carcinomas with axillary lymph node metastases have a 10-year recurrence rate approaching 70%.[2] However, in patients with lymph node negative breast carcinoma, there are no markers used to predict outcome that consistently show statistical significance. In this group, predicting a worse outcome is of great importance, because as many as 20% of women with lymph node negative breast carcinoma eventually will die of metastatic disease.[3] Numerous prognostic markers have been tested to try to predict outcome in this group. In large studies with long follow-up, the best predictors of outcome were tumor size, tumor grade, cathepsin-D expression, Ki-67 expression, S-phase fraction, mitotic index, and vascular invasion. However, despite their marginal statistical status, tumor size and tumor grade enjoy broad acceptance as prognostic factors this group of patients.[4]

Tyrosine kinase receptors (RTKs) are gaining attention as prognostic markers and as possible future predictive markers as the number of trials grows for biospecific inhibitors. Among these, HER-2 (*erb* B2 and *neu*), epidermal growth factor receptor (EGFR), and Met (c-met) have been documented as prognostically significant markers for invasive breast carcinomas predicting a worse prognosis. HER-2 has been associated with outcome in patients with lymph node positive tumors but has not proven valuable in patients with lymph node negative tumors.[5] Although some studies have suggested that EGFR is valuable,[6] EGFR has been examined in over 25 studies, of which only approximately 50% suggest that overexpression is associated with poor outcome.[7] Met has also shown mixed results. Although we and others have found Met useful in predicting worse outcome,[8–10] others either have not seen the correlation or have found an opposite correlation.[11] Finally, FGFR has been studied less and has shown no definitive prognostic value for patients with breast carcinoma.[12]

Slide-to-slide standardization is a long-standing problem in immunohistochemistry studies and may be one explanation for the variability seen in the studies described earlier. Tissue microarray technology can eliminate this problem.[13,14] Tissue microarrays are a method of placing very small samples of tissue from hundreds or thousands of patients on a single slide.[15,16] The technology has been used extensively and is the subject of multiple reviews.[14,17,18] Tissue microarrays are suited especially well to comparisons of expression between multiple prognostic markers. In this report, we revisit the issue of the prognostic value of four RTKs in patients with lymph node negative breast carcinoma with an emphasis on the correlation between the markers. We studied expression patterns of Met, EGFR, fibroblast growth factor receptor (FGFR), and HER-2/*neu* on a cohort of patients with long-term follow-up.

MATERIALS AND METHODS

Tissue Microarray Construction

The tissue microarrays were constructed as described previously[16] and as reviewed recently.[14] Briefly, formalin fixed, paraffin embedded tissue blocks containing breast carcinoma specimens were retrieved from the archives of the Yale University Department of Pathology. Areas of invasive carcinoma were identified on corresponding hematoxylin and eosin-stained slides, and the tissue blocks were cored and transferred to a recipient master block using a Tissue Microarrayer (Beecher Instruments, Sun Prairie, WI). Each core measured 0.6 mm in greatest dimension, and cores were spaced 0.8 mm apart. After cutting the recipient block and transfer with an adhesive tape to coated slides for subsequent ultraviolet cross linkage (Instrumedics, Inc., Hackensack, NJ), the slides were dipped in a layer of paraffin to prevent oxidation. The array for the cohort of patients with lymph node negative breast carcinoma was constructed from paraffin embedded, formalin fixed tissue blocks from the Yale University Department of Pathology archives. The specimens were resected between 1962 and 1980, with a follow-up that ranged between 4 months and 53.8 years, with a mean follow-up of 15.6 years and a median follow-up of 14.3 years.

Grading

Nuclear grade was evaluated by one observer (I.T.O.) according to the methods described by Fisher et al.[19] on each spot. Due to the age of the specimens, they were not assigned a nuclear grade previously. Presence or absence of necrosis, mitotic count, or histologic parameters could not be included in the grading criteria because of the small size of the area evaluated. Eighty of 306 included specimens (26%) were Grade 1, 170 specimens (56%) were Grade 2, and 56 specimens (18%) were Grade 3. Similar to previous studies of nuclear grade in lymph node negative tumors, no statistical significance was achieved. However, a trend was seen between high nuclear grade and worse outcome (5-year survival).

Tumor Size

Information regarding tumor size was obtained from descriptions in the original pathology reports. For staging in the statistical analyses, tumor size $>$ 2.0 cm

was considered *large*, and others were considered *small*.

Immunohistochemistry

The tissue microarray slides were deparaffinized with xylene rinses and then transferred through two changes of 100% ethanol. Endogenous peroxidase activity was blocked by a 30-minute incubation in a 2.5% hydrogen peroxide/methanol buffer. Antigen retrieval was performed by boiling the slides in a pressure cooker filled with a sodium citrate buffer, pH 6.0. After antigen retrieval, the slides were incubated with 0.3% bovine serum albumin/1 × Tris-buffered saline (TBS) for 1 hour at room temperature to reduce nonspecific background staining, followed by a series of 2-minute rinses in 1 × TBS, TBS/0.01% Triton, and 1 × TBS. Primary antibody was applied for 1 hour at room temperature. Dilutions for the RTKs were as follows: Met, 1:1 (note that this antibody was provided as a culture supernate from Zymed Laboratories, Inc., South San Francisco, AC); EGFR, 1:200; FGFR, 1:300; and HER-2, 1:8000. After a series of TBS rinses, as described above, bound antibody was detected by using an antirabbit, horseradish peroxidase-labeled, polymer secondary antibody from the DAKO Envision TM + System (DAKO, Carpinteria, CA). The slides were rinsed in the TBS series and visualized with a 10-minute incubation of liquid 3,3′-diaminobenzidine in buffered substrate (DAKO) for 10 minutes. Finally, the slides were counterstained with hematoxylin and mounted with Immunomount (Shandon, Pittsburgh, PA). Immunohistochemical staining also was done for estrogen receptor (ER), progesterone receptor (PR), and HER-2, as described previously.[20] Ki-67 expression was assessed using purified antihuman monoclonal antibody (1:200 dilution; overnight incubation; Pharmingen, San Diego, CA). The Met antibody 3D4 was provided as part of a collaborative arrangement with Zymed Laboratories, Inc.; the EGFR antibody was EGFR 1005 (catalog no. SC03) from Santa Cruz Biotechnology, Inc. (Santa Cruz, CA); and the FGFR1 antibody was FLG C15 (catalog no. SC121; Santa Cruz Biotechnology, Inc.).

Evaluation of Immunohistochemical Staining

For each spot, the regions of most intense and/or predominant staining pattern were scored by eye. Traditionally, immunohistochemistry scoring of stain intensity includes a variable for the area percentage stained with the specimen; however, due to the small size of the spot (0.6 mm in greatest dimension) and the fact that the spots often are homogenous, no area variable was included. Nuclear staining and/or cytoplasmic staining (ER/PR, EGFR, FGFR, Ki-67, and Met cytoplasmic domains) were determined separately for each specimen. The staining intensity was graded on the following scale: 0, no staining; 1, weak staining; 2, moderate staining; and 3, intense staining. The membranous staining was determined for HER-2 and EGFR. The staining intensity for membranous staining was graded on the following scale: 0, no staining; 1, incomplete staining; 2, weak but complete staining of the plasma membrane encircling the entire cell; and 3, intense complete staining. Again, we did not take the percentage of cells with staining in consideration because of the small size of the tumor sections. For specimens that were uninterpretable, a score of *not available* was given. Only FGFR showed distinctly separate nuclear and cytoplasmic staining characteristics; and, for this antibody, nuclear staining and cytoplasmic staining were scored individually. Scoring of the tissue microarrays was completed by two independent observers (I.T.O and M.D.F.) for EGFR, FGFR nuclear staining, FGFR cytoplasmic staining, and Met with a very high correlation between scorers ($P < 0.0001$). For the antibodies with established staining characteristics in the literature (ER, PR, HER-2, and Ki-67), scoring was performed by one observer (I.T.O. or M.D.F.). Ki-67 was considered positive if > 10% of nuclei were stained. Frequency distributions for these markers were in the range of other works seen in the literature, validating this cohort (see Table 1).

TABLE 1
Distribution of the Expression of Standard Prognostic Markers in the Cohort on Tissue Microarray

Score[a]	ER	PR	HER-2	Ki-67
Positive (%)	57	52	14	60
Negative (%)	43	48	86	40

ER: estrogen receptor; PR: progesterone receptor.
[a] For a description of ordinal scoring of expression and the selection of cut-off values to define positive staining for each marker, see text.

Statistical Analysis

All analyses were completed using Statview software (version 5.0.1; SAS Institute Inc., Cary, NC). The correlation between the scores of both scorers and the relations among the different immunohistochemical and clinicopathologic parameters were measured using the chi-square test. The prognostic significance of parameters on overall survival was calculated by multivariate analysis using a Cox proportional hazards model. Survival curves were calculated using the Kaplan–Meier survival analysis method with the differences estimated using the Mantel–Cox log-rank test.

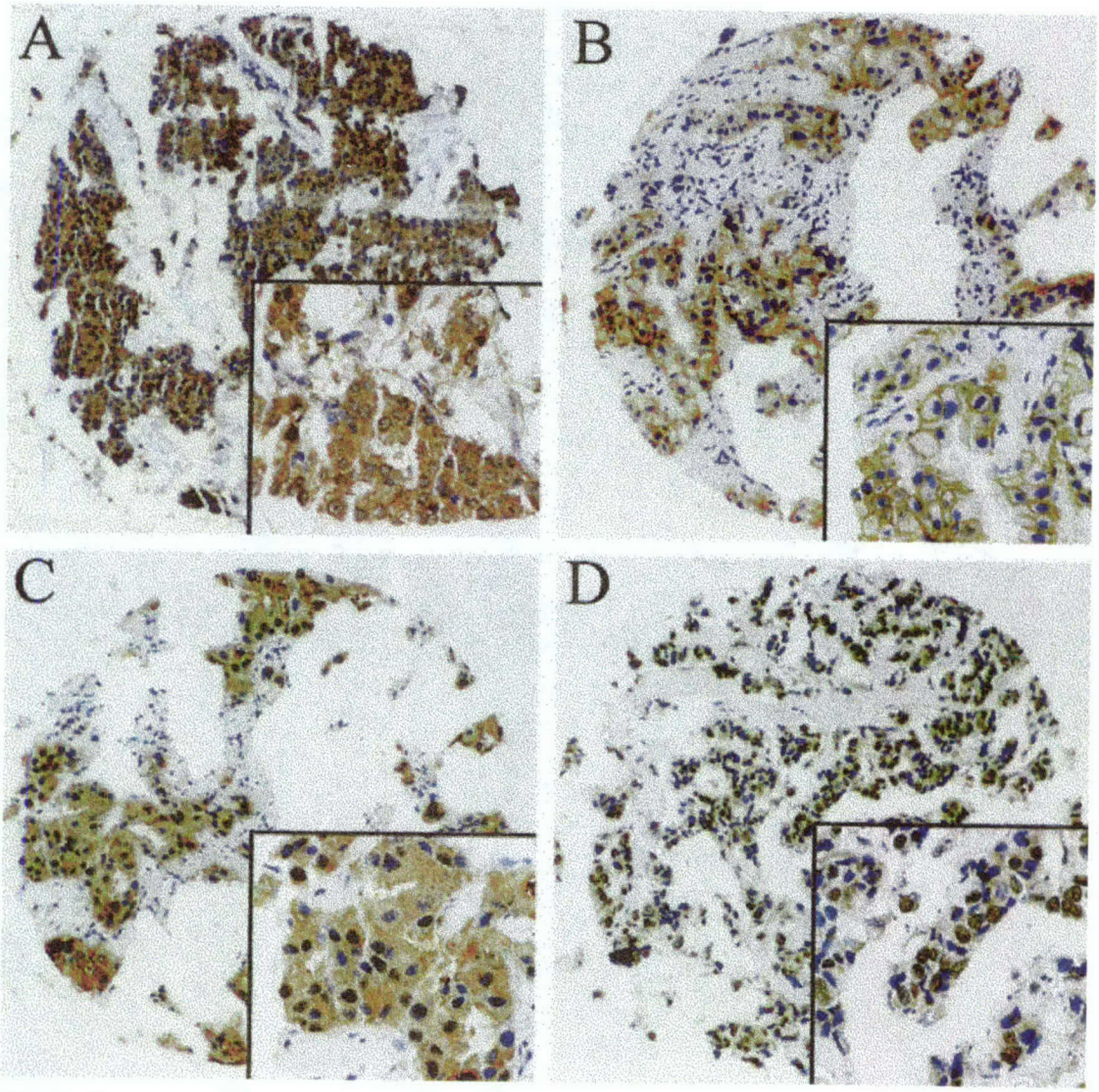

FIGURE 1. Examples of the tissue microarray immunostains for high-level staining (3 +) for Met (A), epidermal growth factor receptor (B), fibroblast growth factor receptor (FGFR) cytoplasmic staining (C), and FGFR nuclear staining (D).

RESULTS

The RTKs analyzed in this study showed a variety of staining patterns that are summarized in Figure 1. Although all RTKs are present at the membrane, there are now numerous studies showing that RTKs can be found in other locations in the cell, including both the cytoplasm and, more recently, the nucleus.[21] The patterns we saw included both conventional membranous patterns as well as both cytoplasmic and nuclear staining (for a detailed description, see above). The pattern of expression of each RTK was determined after examining the entire array to determine the most prevalent patterns. The question of how to divide subjective ordinal staining patterns always is controversial. In this study, we tried to use breakpoints suggested previously in the literature when they were present[8,10]; however, in some instances (FGFR), there were not clear precedents in the literature or the literature was inconsistent (EGFR). A summary of the expression pattern of each RTK is shown in Table 2 with the definition of the cut-off values.

In this study, we were concerned primarily with the correlation between each RTK and the correlation of each RTK with known prognostic markers. We calculated chi-square P values to determine the correlation among expression patterns of individual parameters. Table 3 shows the chi-square P values for all parameters studied in patients with lymph node neg-

TABLE 2
Distribution of Receptor Tyrosine Kinase Expression on Tissue Microarray

Score[a]	HER-2	EGFR	FGFR-n	FGFR-c	Met-c
Positive (%)	14	10.5	48	68	22
Negative (%)	86	89.5	52	32	78

EGFR: epidermal growth factor receptor; FGFR-n: fibroblast growth factor receptor (FGFR) nuclear staining; FGFR-c: FGFR cytoplasmic staining; Met-c: Met cytoplasmic domain.
[a] For definitions for ordinal scoring of expression and the selection of cut-off values to define positive staining for each marker generally are consistant with the literature on these markers. Specifically, for Met, very strong staining was considered positive (3 +), and weak staining (1 + or 2 +) or the absence of staining (0) was considered negative. For HER-2, epidermal growth factor receptor, and fibroblast growth factor receptor, the literature defines 2 + and 3 + as positive and 1 + or 0 as negative.

ative breast carcinoma. Of particular note are the highly significant correlations in immunohistochemical expression patterns of HER-2 and EGFR and of Met and FGFR cytoplasmic staining ($P < 0.0001$). ER expression was correlated highly with PR expression, and they both showed a significant, inverse correlation with HER-2 expression.

Survival Analyses

Cox univariate analyses at 10 years for all variables studied in patients with lymph node negative breast carcinoma are shown in Table 4. Ki-67 and tumor size, as expected, were correlated with poorer survival (Ki-67: $P = 0.04$; relative risk [RR], 1.648; tumor size: $P = 0.0008$; RR, 2.201). Among the other variables studied, only the cytoplasmic domain of Met showed a statistically significant correlation with a worse prognosis and shortened survival ($P = 0.0035$; RR, 2.041). Survival curves were produced for each variable, but only Met reached statistical significance using the Mantel–Cox log-rank test (Fig. 2). To determine the independent predictive value of Met expression, a multivariate analysis was conducted using the Cox proportional hazards model. In multivariate analysis, Met retained its significance as a predictor of worse outcome, even when the model contained all of the conventional prognostic variables as well as all other RTKs tested (RR, 1.86; $P = 0.011$).

DISCUSSION

In patients with lymph node negative breast carcinoma, we still are unable to discern the 15–20% of patients who eventually will succumb to their disease.[3,22] A long list of potential molecular markers of poorer prognosis have been suggested for this group patients with breast carcinoma, including Ki-67,[23,24] cathepsin-D,[25] HER-2,[23,26–28] p53,[27,29] low levels of nm23,[30] and hormone receptors.[24,27,31] There also are reports that histologic findings (e.g., tumor grade, tumor size, mitotic index, and vascular invasion) and cytometric data (e.g., DNA ploidy and S-phase fraction) are helpful.[23,24,27,31–35] To date, there are no universally accepted markers for this group of patients.

We evaluated our tissue microarray cohort using these traditional markers for breast carcinoma. Hormone receptors showed similar staining patterns and frequencies compared with the widely reported values in breast carcinoma. ER was negative in 35% of patients, and PR was negative in 40% of patients. Neither ER expression nor PR expression was predictive of survival in our group. This finding is consistent with many other published studies showing limited value or no value for ER and PR as prognostic markers in patients with lymph node negative breast carcinoma.[30,36] HER-2 has been proven as a predictor of worse prognosis in patients with invasive, lymph node positive breast lesions and is a better predictor of survival compared with hormone receptors for this group of patients.[37] However, its prognostic value in patients with lymph node negative lesions remains controversial, with conflicting data in the literature.[23,26–28] Our findings appear to support the hypothesis that HER-2 is not a reliable prognostic marker in this group of patients.

EGFR expression in breast carcinomas has been reported, both in patients with lymph node negative breast carcinoma and in patients with lymph node positive breast carcinoma, as associated with poor prognosis; however, the clinical significance and association with disease free survival (DFS) and overall survival statistics show mixed results in different studies.[38–40] Tsutsui et al. reported that EGFR carries a prognostic significance only for DFS in patients with lymph node negative tumors on multivariate analysis; whereas, in the series by Torregrosa et al., EGFR failed to show statistical significance as a prognostic marker in patients with lymph node negative tumors but was associated with a worse prognosis, influencing DFS in patients with lymph node positive tumors. Conversely, Seshadri et al. concluded that the expression of EGFR was not at all a predictor of poor prognosis in patients with lymph node negative breast carcinoma. Our findings did not show any value for EGFR as a marker of prognosis in patients with lymph node negative tumors.

Our group has been particularly interested in the hepatocyte growth factor receptor, Met (or C-met). Met is a dimeric tyrosine kinase growth factor receptor in which activation is associated with increased invasion, motogenesis, and morphogenesis.[41] In the breast, Met is expressed in normal ductal and lobular

TABLE 3
Chi-Square Analysis of the Correlation between Expression Levels of Each Marker[a]

Marker	ER	PR	HER-2	EGFR	FGFR-c	FGFR-n	MET	KI-67
ER	—	—	—	—	—	—	—	—
PR	< 0.0001	—	—	—	—	—	—	—
HER-2	0.0003[b,c]	0.0011[b,c]	—	—	—	—	—	—
EGFR	0.0016[b,c]	0.0010[b,c]	< 0.0001[b]	—	—	—	—	—
FGFR-c	0.17	0.24	0.096	0.35	—	—	—	—
FGFR-n	0.90	0.17	0.074	0.11	0.001[b]	—	—	—
MET	0.019[b,c]	0.19	0.54	0.77	< 0.0001[b]	0.12	—	—
KI-67	0.55	0.028[b,c]	0.038[b]	0.053	0.007[b]	0.26	0.03[b]	—
Nuclear grade	0.01[b,c]	0.017[b,c]	0.019[b]	0.0475[b]	0.065	0.0016[b]	< 0.0001[b]	< 0.0001[b]

ER: estrogen receptor; PR: progesterone receptor; EGFR: epidermal growth factor receptor; FGFR-c: fibroblast growth factor receptor (FGFR) cytoplasmic staining; FGFR-n: FGFR nuclear staining.
[a] Statistical analyses of correlation patterns among the parameters studied in patients with lymph node negative breast carcinoma (n = 324 patients).
[b] Statistically significant.
[c] Inverse correlation.

TABLE 4
Univariate Analysis of Conventional and Receptor Tyrosine Kinase Markers

Marker	RR	*P* value	95% CI
ER	1.031	0.9042	0.632–1.681
PR	0.946	0.8184	0.587–1.522
HER-2	1.118	0.7236	0.603–2.071
EGFR	1.029	0.9400	0.494–2.141
FGFR-c	1.078	0.7456	0.685–1.695
FGFR-n	1.338	0.2200	0.840–2.129
MET	2.041[a]	0.0035[a]	1.264–3.295[a]
Ki-67	1.648[a]	0.0418[a]	1.019–2.665[a]
Nuclear grade	1.033	0.9120	0.578–1.846
Tumor size	2.201[a]	0.0008[a]	1.391–3.481[a]

95% CI: 95% confidence interval; ER: estrogen receptor; PR: progesterone receptor; EGFR: epidermal growth factor receptor; FGFR-c: fibroblast growth factor receptor (FGFR) cytoplasmic staining; FGFR-n: FGFR nuclear staining.
[a] Statistically significant.

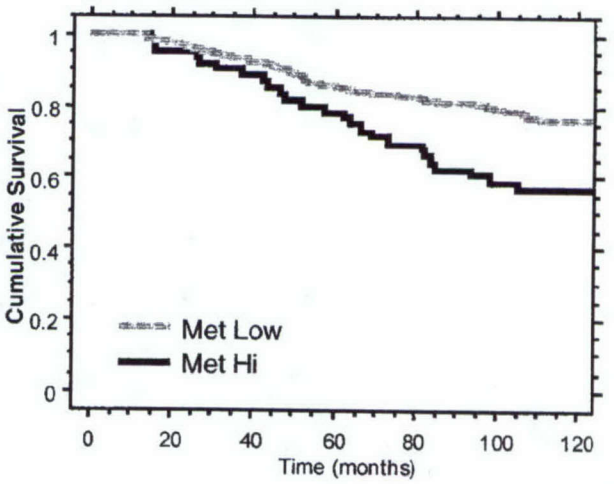

FIGURE 2. Kaplan–Meier survival analysis demonstrates that Met expression, as assessed by antibodies to the cytoplasmic domain, has significant predictive value for the survival of patients with breast carcinoma ($P = 0.0029$; Mantel–Cox log-rank test). Time is indicated in months.

epithelium and functions in both the embryonic development and subsequent remodeling of the breast.[42]

Our previous studies showed that expression of the Met receptor in patients with invasive breast carcinoma is of significant prognostic value in determining patient survival, even in patients with negative lymph nodes.[8,9] The Vande Woude group also found this correlation between Met expression and outcome;[10] although, along with others, we found no correlation in some cohorts (unpublished data). We believe this variability is due to antibody selection. Many studies have used antibodies to the c-terminal domain produced by Santa Cruz Biotechnology, Inc., using a peptide coding for the C-terminal 28 amino acids. We found significant lot-to-lot variability with this antibody. Recently, Zymed Laboratories, Inc. and others have produced monoclonal antibodies to the C-terminus. In another study from our laboratory,[43] we compared the results from this antibody with another monoclonal antibody to the extracellular domain of Met. We showed results with the cytoplasmic domain similar to the results reported here, but the extracellular domain was very different. Although there is a high correlation of expression, overexpression, as assessed by the antibody to the cytoplasmic domain, selects a group of patients with worse outcome, whereas the extracellular domain antibody does not.[43] We believe this may be a function of either cleavage or activation of Met. It is notable that the other study that found a correlation between Met expression and patient outcome also used a monoclonal antibody (generated by the Vande Woude laborato-

ry)[10] and that our own previous studies used a polyclonal antibody made to a cytoplasmic domain peptide.[8]

The finding that Met overexpression predicts poor outcome raises the question of its relation to other RTKs, especially EGFR and HER-2, which also have been implicated as prognostic variables. The current work shows that tumors that overexpress Met are unique from tumors that express HER-2 and EGFR. EGFR and HER-2 are closely related members of the *erb* B oncogene family; thus, it is not surprising that there is a high correlation between the expression of these two proteins. Met is not a member of this family; thus, its overexpression appears to be unrelated to *erb* B family RTKs.

Although there is not a close correlation between Met and the erbB family of RTKs, there is a tight, direct correlation between Met expression and the cytoplasmic staining pattern seen with the FGFR antibody ($P < 0.0001$). To our knowledge, the correlation between FGFR and Met has never been reported before in patients with breast carcinoma. Coordinated actions of several growth factors and their receptors, including FGFR and C-met, have been reported in patients with hepatic lesions[44] and in normal morphogenesis in the uterus;[45] however, the molecular basis of such an interaction, if present, remains unknown. Although FGFR is a membrane-based RTK, immunohistochemical evaluation for FGFR has not been standardized as a marker for immunohistochemistry. Thus, we scored cytoplasmic and nuclear staining for FGFR separately. Although neither cytoplasmic staining for FGRF nor nuclear staining for FGFR was a statistically significant prognostic marker in our study, there was a high correlation between Met expression and FGFR cytoplasmic expression.

RTKs recently have gained great interest both as markers of prognosis and as promising targets for novel chemotherapeutic options. The HER2/trastuzmab pair is the first U.S. Food and Drug Administration-approved example of numerous RTK-related therapeutics currently in clinical trials. This interest raises the question of the relations between different RTKs. Although data on the cross reactivity of kinase-based therapeutics is not widely available to date, there are many of types of RTK receptors that are overexpressed in malignancies of the breast.

The results of the current study indicate that the expression of Met, as assessed using a cytoplasmic domain monoclonal antibody, in patients with lymph node negative, invasive breast carcinoma is of significant predictive value in determining patient survival. Its predictive value exceeds all conventional prognostic markers assessed in this cohort as well as the other RTKs tested. The group of patients that overexpress this protein are unrelated to the group that overexpresses either EGFR or HER-2. Thus, in the future, determination of prognosis in patients with lymph node negative, invasive breast carcinoma may be improved by assessment of the level of expression of Met using a cytoplasmic domain monoclonal antibody.

REFERENCES

1. Fitzgibbons PL, Page DL, Weaver D, et al. Prognostic factors in breast cancer. College of American Pathologists consensus statement 1999. *Arch Pathol Lab Med.* 2000;124:966–978.
2. Elledge RM, McGuire WL. Prognostic factors and therapeutic decisions in axillary node-negative breast cancer. *Annu Rev Med.* 1993;44:201–210.
3. Fisher ER, Costantino J, Fisher B, Redmond C. Pathologic findings from the National Surgical Adjuvant Breast Project (Protocol 4). Discriminants for 15-year survival. National Surgical Adjuvant Breast and Bowel Project Investigators. *Cancer.* 1993;71:2141–2150.
4. Mirza AN, Mirza NQ, Vlastos G, Singletary SE. Prognostic factors in node-negative breast cancer: a review of studies with sample size more than 200 and follow-up more than 5 years. *Ann Surg.* 2002;235:10–26.
5. Lohrisch C, Piccart M. HER2/*neu* as a predictive factor in breast cancer. *Clin Breast Cancer.* 2001;2:129–137.
6. Pawlowski V, Revillion F, Hebbar M, Hornez L, Peyrat JP. Prognostic value of the type I growth factor receptors in a large series of human primary breast cancers quantified with a real-time reverse transcription-polymerase chain reaction assay. *Clin Cancer Res.* 2000;6:4217–4225.
7. Nicholson RI, Gee JM, Harper ME. EGFR and cancer prognosis. *Eur J Cancer.* 2001;37(Suppl 4):S9–S15.
8. Camp RL, Rimm EB, Rimm DL. Met expression is associated with poor outcome in patients with axillary lymph node negative breast carcinoma. *Cancer.* 1999;86:2259–2265.
9. Ghoussoub RA, Dillon DA, D'Aquila T, Rimm EB, Fearon ER, Rimm DL. Expression of c-met is a strong independent prognostic factor in breast carcinoma. *Cancer.* 1998;82:1513–1520.
10. Tsarfaty I, Alvord WG, Resau JH, et al. Alteration of Met protooncogene product expression and prognosis in breast carcinomas. *Anal Quant Cytol Histol.* 1999;21:397–408.
11. Nakopoulou L, Gakiopoulou H, Keramopoulos A, et al. c-met tyrosine kinase receptor expression is associated with abnormal beta-catenin expression and favourable prognostic factors in invasive breast carcinoma. *Histopathology.* 2000;36:313–325.
12. Dickson C, Spencer-Dene B, Dillon C, Fantl V. Tyrosine kinase signalling in breast cancer: fibroblast growth factors and their receptors. *Breast Cancer Res.* 2000;2:191–196.
13. Torhorst J, Bucher C, Kononen J, et al. Tissue microarrays for rapid linking of molecular changes to clinical endpoints. *Am J Pathol.* 2001;159:2249–2256.
14. Rimm DL, Camp RL, Charette LA, Costa J, Olsen DA, Reiss M. Tissue microarray: a new technology for amplification of tissue resources. *Cancer J.* 2001;7:24–31.
15. Wan WH, Fortuna MB, Furmanski P. A rapid and efficient method for testing immunohistochemical reactivity of monoclonal antibodies against multiple tissue samples simultaneously. *J Immunol Methods.* 1987;103:121–219.

16. Kononen J, Bubendorf L, Kallioniemi A, et al. Tissue microarrays for high-throughput molecular profiling of tumor specimens. *Nat Med.* 1998;4:844–847.
17. Bubendorf L, Nocito A, Moch H, Sauter G. Tissue microarray (TMA) technology: miniaturized pathology archives for high-throughput in situ studies. *J Pathol.* 2001;195:72–79.
18. Skacel M, Skilton B, Pettay JD, Tubbs RR. Tissue microarrays: a powerful tool for high-throughput analysis of clinical specimens: a review of the method with validation data. *Appl Immunohistochem Mol Morphol.* 2002;10:1–6.
19. Fisher ER, Redmond C, Fisher B. Histologic grading of breast cancer. *Pathol Annu.* 1980;15:239–251.
20. Camp RL, Charette LA, Rimm DL. Validation of tissue microarray technology in breast carcinoma. *Lab Invest.* 2000; 80:1943–1949.
21. Lin SY, Makino K, Xia W, et al. Nuclear localization of EGF receptor and its potential new role as a transcription factor. *Nat Cell Biol.* 2001;3:802–808.
22. Carter CL, Allen C, Henson DE. Relation of tumor size, lymph node status, and survival in 24,740 breast cancer cases. *Cancer.* 1989;63:181–187.
23. Rudolph P, Olsson H, Bonatz G, et al. Correlation between p53, c-erbB-2, and topoisomerase II alpha expression, DNA ploidy, hormonal receptor status and proliferation in 356 node-negative breast carcinomas: prognostic implications. *J Pathol.* 1999;187:207–216.
24. Seshadri R, Leong AS, McCaul K, Firgaira FA, Setlur V, Horsfall DJ. Relationship between p53 gene abnormalities and other tumour characteristics in breast-cancer prognosis. *Int J Cancer.* 1996;69:135–141.
25. Foekens JA, Look MP, Bolt-de Vries J, Meijer-van Gelder ME, van Putten WL, Klijn JG. Cathepsin-D in primary breast cancer: prognostic evaluation involving 2810 patients. *Br J Cancer.* 1999;79:300–307.
26. Sjogren S, Inganas M, Lindgren A, Holmberg L, Bergh J. Prognostic and predictive value of c-erbB-2 overexpression in primary breast cancer, alone and in combination with other prognostic markers. *J Clin Oncol.* 1998;16:462–469.
27. Reed W, Hannisdal E, Boehler PJ, Gundersen S, Host H, Marthin J. The prognostic value of p53 and c-erb B-2 immunostaining is overrated for patients with lymph node negative breast carcinoma: a multivariate analysis of prognostic factors in 613 patients with a follow-up of 14–30 years. *Cancer.* 2000;88:804–813.
28. Press MF, Bernstein L, Thomas PA, et al. HER-2/*neu* gene amplification characterized by fluorescence in situ hybridization: poor prognosis in node-negative breast carcinomas. *J Clin Oncol.* 1997;15:2894–2904.
29. Silvestrini R, Benini E, Daidone MG, et al. p53 as an independent prognostic marker in lymph node-negative breast cancer patients. *J Natl Cancer Inst.* 1993;85:965–970.
30. Barnes R, Masood S, Barker E, et al. Low nm23 protein expression in infiltrating ductal breast carcinomas correlates with reduced patient survival. *Am J Pathol.* 1991;139: 245–250.
31. Fisher B, Redmond C, Fisher ER, Caplan R. Relative worth of estrogen or progesterone receptor and pathologic characteristics of differentiation as indicators of prognosis in node negative breast cancer patients: findings from National Surgical Adjuvant Breast and Bowel Project Protocol B-06. *J Clin Oncol.* 1988;6:1076–1087.
32. Rosen PR, Groshen S, Saigo PE, Kinne DW, Hellman S. A long-term follow-up study of survival in Stage I (T1N0M0) and Stage II (T1N1M0) breast carcinoma. *J Clin Oncol.* 1989; 7:355–366.
33. Railo M, Lundin J, Haglund C, von Smitten K, von Boguslawsky K, Nordling S. Ki-67, p53, Er-receptors, ploidy and S-phase as prognostic factors in T1 node negative breast cancer. *Acta Oncol.* 1997;36:369–374.
34. Balslev I, Christensen IJ, Rasmussen BB, et al. Flow cytometric DNA ploidy defines patients with poor prognosis in node-negative breast cancer. *Int J Cancer.* 1994;56:16–25.
35. Aaltomaa S, Lipponen P, Eskelinen M, et al. Mitotic indexes as prognostic predictors in female breast cancer. *J Cancer Res Clin Oncol.* 1992;118:75–81.
36. Fisher ER, Redmond C, Fisher B. Prognostic factors in NSABP studies of women with node-negative breast cancer. National Surgical Adjuvant Breast and Bowel Project. *J Natl Cancer Inst Monogr.* 1992:151–158.
37. Slamon DJ, Clark GM, Wong SG, Levin WJ, Ullrich A, McGuire WL. Human breast cancer: correlation of relapse and survival with amplification of the HER-2/*neu* oncogene. *Science.* 1987;235:177–182.
38. Torregrosa D, Bolufer P, Lluch A, et al. Prognostic significance of c-erbB-2/*neu* amplification and epidermal growth factor receptor (EGFR) in primary breast cancer and their relation to estradiol receptor (ER) status. *Clin Chim Acta.* 1997;262:99–119.
39. Tsutsui S, Ohno S, Murakami S, Hachitanda Y, Oda S. Prognostic value of epidermal growth factor receptor (EGFR) and its relationship to the estrogen receptor status in 1029 patients with breast cancer. *Breast Cancer Res Treat.* 2002;71: 67–75.
40. Seshadri R, McLeay WR, Horsfall DJ, McCaul K. Prospective study of the prognostic significance of epidermal growth factor receptor in primary breast cancer. *Int J Cancer.* 1996; 69:23–27.
41. Comoglio PM, Boccaccio C. Scatter factors and invasive growth. *Semin Cancer Biol.* 2001;11:153–165.
42. Niranjan B, Buluwela L, Yant J, et al. HGF/SF: a potent cytokine for mammary growth, morphogenesis and development. *Development.* 1995;121:2897–2908.
43. Kang JY, Dolled-Filhart M, Ocal IT, et al. Tissue microarray analysis of hepatocyte growth factor Met pathway components reveals a role for Met, Matriptase, and Hepatocyte growth factor activator inhibitor 1 in the progression of node-negative breast cancer. *Cancer Res* 2003;63:1101–1105.
44. Hu Z, Evarts RP, Fujio K, et al. Expression of transforming growth factor alpha/epidermal growth factor receptor, hepatocyte growth factor/c-met and acidic fibroblast growth factor/fibroblast growth factor receptors during hepatocarcinogenesis. *Carcinogenesis.* 1996;17:931–938.
45. Taylor KM, Chen C, Gray CA, Bazer FW, Spencer TE. Expression of messenger ribonucleic acids for fibroblast growth factors 7 and 10, hepatocyte growth factor, and insulin-like growth factors and their receptors in the neonatal ovine uterus. *Biol Reprod.* 2001;64:1236–1246.

[CANCER RESEARCH 63, 1445–1448, April 1, 2003]

Appendix 4

Advances in Brief

Quantitative Analysis of Breast Cancer Tissue Microarrays Shows That Both High and Normal Levels of HER2 Expression Are Associated with Poor Outcome[1]

Robert L. Camp,[2] Marisa Dolled-Filhart, Bonnie L. King, and David L. Rimm

Departments of Pathology [R. L. C., D. L. R.], Genetics [M. D-F.], and Therapeutic Radiology [B. L. K.], Yale University, School of Medicine, New Haven, Connecticut 06520

Abstract

Using a tissue microarray cohort of 300 breast cancers and 84 samples of normal breast epithelium, we analyzed HER2/*neu* expression and compared traditional clinical (manual) scoring with a recently developed system for the quantitative measurement of immunohistochemical stains (AQUA). As expected, both methods identified a population (10–15%) of high-HER2-expressing tumors with poor 30-year disease-related survival. Using AQUA analysis, we found that normal epithelium expresses a low but detectable level of HER2 and that 17.5% of tumors exhibit similar low-level HER2 expression. This low group was not definable by manual scoring. Surprisingly, HER2-normal tumors were as aggressive as HER2-overexpressing tumors. Our studies suggest that *in situ* quantitative measurement of HER2 stratifies breast tumors into three expression levels: normal, intermediate, and high, where both normal and high levels are associated with a worse outcome.

Introduction

HER2 (*neu* or erb-B2), a member of the epidermal growth factor family, is genetically amplified and overexpressed in aggressive breast cancers. High levels of HER2 are associated with poor prognosis, particularly in node-positive breast carcinoma patients. Recently, a targeted therapeutic against HER2 has been developed. Trastuzumab (Herceptin) is a humanized monoclonal antibody directed against the extracellular domain of HER2. Treatment of patients with metastatic breast carcinoma with Herceptin has shown therapeutic benefit, especially when combined with conventional chemotherapeutic agents. The association between HER2 expression and Herceptin response has stimulated renewed interest in accurately assessing HER2 amplification and overexpression. Toward this goal, we have developed a system for compartmentalized, automated quantitative analysis of histological sections (AQUA; Ref. 1). As with an ELISA, AQUA provides highly reproducible analysis of target signal expression with use of a continuous, rather than nominal, scale. Unlike an ELISA, spatial information, including tissue and subcellular localization, is preserved. Using a tissue microarray composed of archival breast cancer specimens and normal epithelia, we found a bimodal distribution of HER2, where tumors expressing both high and normal HER2 levels exhibited poor 30-year disease-specific survival.

Materials and Methods

Tissue Microarray Design. Paraffin-embedded, formalin-fixed specimens from 300 cases of node-positive invasive breast carcinoma were identified from the archives of the Yale University Department of Pathology as available from 1962 to 1977, with a mean follow-up time of 9.6 years. No patients received Herceptin during the study period. Complete treatment information was unavailable for the entire cohort; however, most patients were treated with local radiation and ~15% were treated with chemotherapy consisting primarily of Adriamycin, cytoxan, and 5-fluorouracil. Approximately 27% subsequently received tamoxifen (post-1978). Seven patients had biopsy-proven stage IV disease at the time of diagnosis.

In constructing the microarrays, we identified areas of invasive carcinoma, away from *in situ* lesions and normal epithelium, and took two 0.6-mm cores. We cut 5-μm-thick sections of the microarrays and processed them as described previously (2, 3). We previously demonstrated with HER2 that two cores replicated the results of an entire slide in >95% of cases (4). An additional microarray consisting of 84 samples of normal epithelium was also constructed from samples of normal ducts and lobules taken from breast cancer patients. Samples were taken away from areas of tumor and assessed histologically to ensure that they were unaffected by atypical hyperplasia or carcinoma *in situ*.

Immunohistochemistry. Tissue microarray slides were stained as described (1). In brief, for both manual and automated analysis, slides were incubated for 1 h at room temperature with polyclonal anti-HER2 (1:200; DAKO Corp., Carpinteria, CA) diluted in Tris-buffered saline containing BSA. Previous analysis of titrations of the HER2 antibody demonstrated that higher dilutions of anti-HER2 antibody (1:1000~1:8000) more accurately define the HER2-high from the HER2-intermediate populations, whereas lower dilutions (1:50~1:500) distinguish the HER2-normal from HER2-intermediate populations.[3] In this study we used a concentration (1:200) that sufficiently distinguished all three populations. Goat antirabbit antibody conjugated to a horseradish peroxidase-decorated dextran polymer backbone (Envision; DAKO Corp.) was used as a secondary reagent. For manual analysis, slides were visualized with diaminobenzidine (DAKO Corp.), followed by ammonium hydroxide-acidified hematoxylin. For automated analysis, tumor cells were identified by use of a fluorescently tagged anticytokeratin antibody cocktail (AE1/AE3; DAKO Corp.). We added 4′,6-diamidino-2-phenylindole to visualize nuclei, and HER2 was visualized with a fluorescent chromogen (Cy-5-tyramide; NEN Life Science Products, Boston, MA). Cy-5 (red) was used because its emission peak is well outside the green-orange spectrum of tissue autofluorescence.

Automated Image Acquisition and Analysis. Automated image acquisition and analysis using AQUA has been described previously (1). In brief, monochromatic, high-resolution (1024 × 1024 pixel; 0.5-μm) images were obtained of each histospot. We distinguished areas of tumor from stromal elements by creating a mask from the cytokeratin signal. Coalescence of cytokeratin at the cell surface helped localize the cell membranes, and 4′,6-diamidino-2-phenylindole was used to identify nuclei. The HER2 signal from the membrane area of tumor cells was scored on a scale of 0–255 and expressed as signal intensity divided by the membrane area.

FISH. FISH[4] analysis was performed with the PathVysion HER2 DNA Probe Kit (Vysis, Downers Grove, IL), using two directly labeled fluorescent DNA probes complementary to the HER2/*neu* gene locus (LSI HER2/*neu* SpectrumRed) and to chromosome 17 pericentromeric α satellite DNA (CEP17 SpectrumGreen), according to standard protocols. HER2/*neu* gene amplification was quantified by comparing the ratio of LSI HER2/*neu* to CEP17 probe signals in accordance with the PathVysion HER2 DNA Probe Kit criteria. We examined 60 nonoverlapping tumor cell nuclei in each histo-

Received 11/6/02; accepted 2/14/03.

The costs of publication of this article were defrayed in part by the payment of page charges. This article must therefore be hereby marked *advertisement* in accordance with 18 U.S.C. Section 1734 solely to indicate this fact.

[1] This work was supported by grants from the Patrick and Catherine Weldon Donaghue Foundation for Medical Research, by grants from the NIH [K0-8 ES11571, NIEHS (to R. L. C.), and RO-1 GM57604 NCI (to D. L. R.)], the Greenwich Breast Cancer Alliance, and by United States Army DAMD Grant 01-000436.

[2] To whom requests for reprints should be addressed, at Department of Pathology, Yale University, School of Medicine, New Haven, CT 06520-8023.

[3] R. L. Camp, M. Dolled-Filhart, D. L. Rimm, unpublished observations.

[4] The abbreviation used is: FISH, fluorescence *in situ* hybridization.

spot to determine the average number of HER2/*neu* and chromosome 17 copies/cell for each tissue specimen. The ratio of these averages was used to determine the presence of HER2/*neu* gene amplification. Specimens with a HER2/*neu*:chromosome 17 ratio >2 were scored as positive for HER2/*neu* gene amplification.

Data Analysis. Manual scoring of HER2 expression was assessed by a pathologist (R. L. C.) using a nominal four-point scale (0 to 3+). Histospots containing <10% tumor, as assessed either subjectively (manual) or by mask area (automated), were excluded from further analysis. Previous studies have demonstrated that the staining from a single histospot provides a sufficiently representative sample for analysis (4, 5). Correlations with other prognostic markers were determined by χ^2 analysis. Overall survival analysis was assessed by Kaplan-Meier analysis with the Mantel-Cox log-rank score for determining statistical significance. Relative risk was assessed by the univariate and multivariate Cox proportional hazards model. Analyses were performed with Statview 5.0.1 (SAS Institute, Cary, NC). Patients were deemed "uncensored" if they died of breast cancer within 30 years of their initial date of diagnosis.

Results and Discussion

Validation of Microarray Cohort. To validate our tissue microarray cohort of 300 node-positive breast cancers, we assessed several traditional histopathological markers of malignancy. Using univariate analysis of long-term disease-related survival, we found that large tumor size, high nuclear grade, low estrogen receptor expression, and high number of involved lymph nodes were all significant predictors of poor outcome (Table 1). We next assessed the prognostic power of HER2 immunohistochemistry, using standard brown staining, visual examination by a pathologist, and scoring on a four-point scale (0 to 3+). Manual analysis showed a typical pattern of HER2 expression with 15% of tumors overexpressing the antigen (2+ and 3+; Fig. 1*B*). As expected, high-level (3+) tumors showed a significantly worse outcome with a relative risk of 2.25 ($P = 0.0007$; Table 1). Analysis of *HER2* gene amplification by FISH was not predictive in our study, but this was most likely attributable to the relatively small number of cases that, for technical reasons, were scorable (125 of 300; Table 1). However, both automated and manual analyses of HER2 protein levels were highly correlated with *HER2* gene amplification ($P < 0.0001$). The percentage of HER2-amplified cases in each manual category were 4.0% (0), 13.7% (1+), 71.4% (2+), and 75.0% (3+), and in each AQUA category were 9.5% (normal), 13.7% (intermediate), and 77.8% (high).

HER2 Expression on Normal Epithelium. We then assessed the level of HER2 expression on normal breast epithelium with use of automated analysis on a microarray. This epithelium was derived from normal ducts and/or lobules isolated from uninvolved breast tissue taken from 84 breast cancer patients. Consistent with previous studies using biochemical assays, our results demonstrated a low but detectable level of HER2 in normal epithelium, which was tightly grouped into a single peak with a mean of 5 and a SD of 1.5 (AQUA score; Fig. 1*A*; Ref. 6).

Table 1 *Univariate analysis of 30-year disease-related survival*

Marker	*n*	*P*	Relative risk	95% confidence interval
HER2 manual score		0.0071		
0	153		1.00	
1+	50	0.9383	1.02	0.68–1.52
2+	13	0.9763	1.01	0.49–2.08
3+	28	0.0007	2.25	1.41–3.58
HER2 AQUA score		0.0009		
Normal	46	0.0091	1.71	1.14–2.56
Intermediate	188		1.00	
High	30	0.0013	2.18	1.35–3.51
HER2 amplification (FISH)	22	0.8121	1.07	0.60–1.90
Nodal involvement		0.0279		
1–3	68		1.00	
4–9	54	0.6708	1.08	0.75–1.55
≥10	141	0.0086	1.62	1.13–2.33
Tumor size (cm)		0.0007		
<2	80		1.00	
2–5	53	0.1255	1.33	0.92–1.93
>5	102	0.0001	2.09	1.43–3.07
Nuclear grade				
High	95	0.0040	1.55	1.15–2.08
Estrogen receptor				
Negative	104	0.0262	1.41	1.041–1.906

Automated Analysis of HER2 Expression in Breast Cancer. In contrast to the tightly grouped peak in normal epithelium, HER2 expression in breast tumors was broadly distributed (Fig. 1*C*). Expression levels of HER2 in tumors exhibited a mode similar to that of normal epithelium, but with significant skew toward higher-level expression. Examination of the histogram suggested that there were three naturally occurring populations based on HER2 expression: normal, intermediate, and high (Fig. 1*C*). A discernible break in the histogram at AQUA score 25 divided HER2-high from the remaining tumors. The remaining tumors could then be subdivided into HER2-low and HER2-intermediate groups depending on whether their expression levels were greater than the mean HER2 expression on normal epithelium + 1 SD (AQUA score <6.5; Fig. 1, *A* and *C*). On the basis of these divisions, 17.5% of the tumors were designated HER2 normal, 71.3% were HER2 intermediate, and 11.2% were HER2 high.

Comparison of Manual and Automated Techniques. We then compared HER2 expression as gauged by automated and manual techniques (Fig. 1, *panels C* and *B*, respectively). In contrast to AQUA scores, which were continuously scored on a scale of 0–255, manual scoring of HER2 expression was performed on a nominal four-point scale (0 to 3+). Despite this difference, regression analysis demonstrated good correlation between the two methods ($r = 0.704$). However, there was a significant degree of overlap in the automated scores of cases from adjacent manually determined groups (Fig. 1*D*). Whereas there was a clear division between the histograms of tumors scoring 0/1+ and 2+/3+, the distinction between tumors scoring 0 and 1+ was indistinct. This result shows the difficulty in manually translating a biological (continuous) marker into a nominal four-point scale. Even for the trained eye of a pathologist, accurate distinction between nominal categories (*e.g.*, 2+ *versus* 3+) is difficult and often arbitrary. Indeed, recent studies have demonstrated a significant lack of reproducibility in the clinical determination of HER2 levels attributable in part to this difficulty (7–9).

Examination of manual and automated techniques revealed that both were equally able to define a population of tumors expressing high levels of HER2 with poor outcome (relative risk, 2.25 and 2.18; $P = 0.0007$ and 0.0013, respectively; Table 1). However, unlike manual analysis, automated analysis revealed that tumors expressing normal levels of HER2 also showed a significantly worse outcome (relative risk, 1.71; $P = 0.0091$; Table 1). Given the amount of overlap in the 0 and 1+ categories from manual scoring (Fig. 1*D*), it is not surprising that manual assessment of stained slides has not previously identified the HER2-normal population.

Defining the Subpopulation of HER2-normal Tumors. To determine whether HER2 expression correlated with known prognostic markers in our cohort, we assessed possible associations between HER2 and hormone receptor status, tumor size, and nuclear grade. High-level HER2 expression was correlated with high nuclear grade and inversely correlated with estrogen receptor status (Table 2).

The HER2-normal population showed no significant correlation with nodal involvement, tumor size, or estrogen receptor, but did show an association with high nuclear grade ($P = 0.0494$; Table 2). Few of the HER2-normal tumors exhibited gene amplification (2 of 21 examined), ruling out the possibility that in tumors expressing

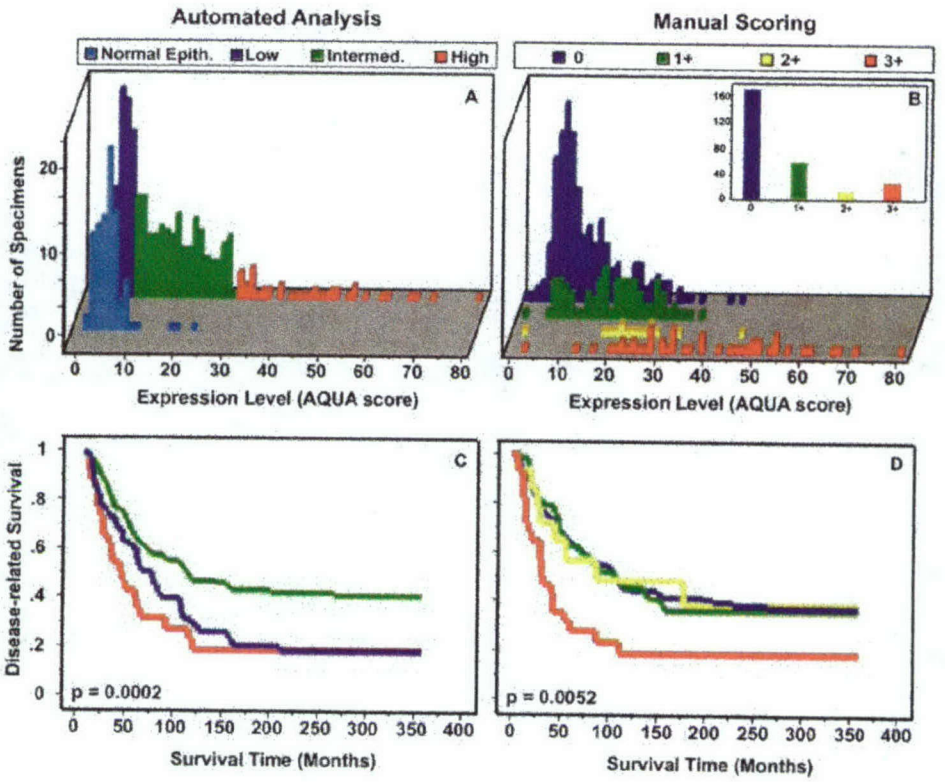

Fig. 1. Automated analysis of HER2 divides tumors into three categories based on their level of expression. *A*, analysis of 84 samples of normal epithelium demonstrates a low but detectable level of HER2 expression (*light blue*). Examination of a cohort of 300 node-positive carcinomas shows a right-skewed histogram (*dark blue*, *green*, and *red*). Cases were divided by expression level as follows: high (AQUA score >25; *red*), normal (AQUA score less than the mean expression of normal epithelium + 1 SD; *dark blue*), and intermediate (between normal and high; *green*). *B*, manual (visual) analysis of HER2 staining using a nominal four-point scale shows that 15% of the tumors over-express HER2 (2+/3+; *inset*). AQUA scores of tumors separated according to their manual score (0 to 3+) show significant overlap, particularly between 0 and 1+ tumors. *C*, Kaplan-Meier analysis of automated HER2 scores shows that both normal and high-level expressers do poorly relative to intermediate-level tumors. *D*, Kaplan-Meier analysis of manual HER2 scores distinguishes a survival difference only with the high (3+) expressers.

normal levels of HER2, the *HER2* gene is amplified but the HER2 protein is not detected.

Multivariate Analysis of HER2-normal and -high Populations. Finally, we determined whether normal or high expression of HER2 by tumors was an independent predictor of long-term disease-related survival. Combined multivariate analysis of HER2 with the traditional histopathological markers, nodal involvement, tumor size, nuclear grade, and estrogen receptor, demonstrated that both normal- and high-level HER2 expression were independently predictive of patient outcome (Table 3).

Our data suggest that HER2 divides cases of node-positive breast carcinoma into three categories: normal, intermediate, and high expressers. Tumors expressing either normal or high HER2 levels do poorly in long-term follow-up. Of particular note are three previous studies that have looked at HER2 expression levels using "gold standard" biochemical techniques (Western blots and ELISAs; Refs. 6, 10–13). Two of these studies suggested a bimodal distribution for HER2, with both low and high levels correlating with known markers of tumor aggression (10–12), but a third found no such distribution (13). Because such techniques require fresh tissue for analysis, they were unable to assess long-term follow-up on a large cohort of patients. The AQUA-based analysis provides quantitative information from tissue microarrays constructed from archival tissues; we thus were able to examine a large cohort of patients with known long-term disease-related survival. Our data show that normal HER2 expression is an independent prognostic indicator of poor outcome and demonstrate that, unlike manual immunohistochemical analysis, automated analysis can identify a patient population that is otherwise detectable only by established biochemical assays.

HER2 overexpression can induce an aggressive phenotype via the activation of downstream regulators (*e.g.*, phosphoinositol 3-kinase, *Erk*/MAP kinase, and *Ras*; Refs. 14–16). How normal levels of HER2 could be associated with a similar aggressive phenotype is unknown at present. We speculate that these tumors might overexpress another growth factor receptor that promotes tumor aggression via a ligand-dependent or -independent mechanism. It is possible that expression

Table 2 *Distribution of prognostic markers by HER2 level based on χ^2 analysis*

Marker	All cases		Normal (%)	Intermediate (%)	High (%)	P (χ^2)	
	n	%				Normal *vs.* intermediate	High *vs.* intermediate
Nodes positive	268					0.8171	0.1891
1–3	145	54	60	54	43		
4–9	70	26	23	27	33		
≥10	53	20	17	19	23		
Tumor size (cm)	238					0.3033	0.8911
<2	102	43	35	44	48		
2–5	81	34	44	32	32		
>5	55	23	21	24	20		
Nuclear grade	269					0.0494	0.0011
High	97	36	45	30	60		
Estrogen receptor	263					0.5325	<0.0001
Negative	105	40	39	34	77		

Table 3 *Multivariate analysis of 30-year disease-related survival*

Marker	*n*	*P*	Relative risk	95% confidence interval
HER2		0.0097		
Normal	42	0.0191	1.68	1.09–2.59
Intermediate	162		1.00	
High	25	0.0136	1.96	1.15–3.36
Nodal involvement		0.1058		
1–3	60		1.00	
4–9	48	0.5915	1.12	0.73–1.72
≥10	121	0.0353	1.61	1.03–2.53
Tumor size (cm)		<0.0001		
<2	78		1.00	
2–5	52	0.2220	1.31	0.85–2.01
>5	99	<0.0001	2.59	1.67–4.02
Nuclear grade				
High	87	0.2158	1.26	0.87–1.82
Estrogen receptor				
Negative	89	0.0032	1.75	1.21–2.54

of such alternate growth factor receptors in some tumors results in the down-regulation of HER2 expression via a feedback mechanism, producing aggressive tumors bearing a HER2-normal phenotype. Another possible explanation for the poor prognosis of HER2-normal tumors is that high levels of coreceptor ligand-independent activation of HER2 might result in the internalization and degradation of the receptor, producing apparent low-level HER2 expression. Finally, HER2-normal breast cancers may represent a population of aggressive poorly differentiated neoplasms that have developed HER2- and growth factor-independent mechanisms for their growth. The association between normal HER2 expression levels and high nuclear grade supports this idea. Recent data from the Brown and Botstein group also support this finding. They showed five unique breast cancer classes by cDNA array clustering experiments, two of which had very poor outcomes. One of these groups was HER2 positive, but the other showed no evidence of HER2 overexpression (17).

From a clinical perspective, response to Herceptin has largely been seen in HER2 high expressers or HER2-amplified cases. This may be attributable to the fact that 2+ or 3+ levels of expression were required for entry into most clinical trials (18–20). The response of 0 or 1+ tumors to paclitaxel with and without Herceptin is being studied in a large randomized trial (CALGB 9840; Ref. 21). Although patients with HER2-normal tumors are unlikely to respond to Herceptin, they may benefit from more aggressive traditional chemotherapy. The ability to accurately distinguish between HER2-normal and HER2-intermediate tumors by automated analysis not only has prognostic value but may also help in the development and evaluation of new therapeutics targeted to treat this subpopulation.

Acknowledgments

We thank Michael DiGiovanna and D. Craig Allred for critical review of this manuscript. We also thank Nicole Parisot, Thomas D'Aquila, Mary Helie, Lori Charette, and Diana Fischer for assistance in this effort.

References

1. Camp, R. L., Chung, G. G., and Rimm, D. L. Automated subcellular localization and quantification of protein expression in tissue microarrays. Nat. Med., *8:* 1323–1328, 2002.
2. Rimm, D. L., Camp, R. L., Charette, L. A., Olsen, D. A., and Provost, E. Amplification of tissue by construction of tissue microarrays. Exp. Mol. Pathol., *70:* 255–264, 2001.
3. Kononen, J., Bubendorf, L., Kallioniemi, A., Barlund, M., Schraml, P., Leighton, S., Torhorst, J., Mihatsch, M. J., Sauter, G., and Kallioniemi, O. P. Tissue microarrays for high-throughput molecular profiling of tumor specimens. Nat. Med., *4:* 844–847, 1998.
4. Camp, R. L., Charette, L. A., and Rimm, D. L. Validation of tissue microarray technology in breast carcinoma. Lab. Investig., *80:* 1943–1949, 2000.
5. Torhorst, J., Bucher, C., Kononen, J., Haas, P., Zuber, M., Kochli, O. R., Mross, F., Dieterich, H., Moch, H., Mihatsch, M., Kallioniemi, O. P., and Sauter, G. Tissue microarrays for rapid linking of molecular changes to clinical endpoints. Am. J. Pathol., *159:* 2249–2256, 2001.
6. Dittadi, R., Donisi, P. M., Brazzale, A., Marconato, R., Spina, M., and Gion, M. Immunoenzymatic assay of erbB2 protein in cancer and non-malignant breast tissue. Relationships with clinical and biochemical parameters. Anticancer Res., *12:* 2005–2010, 1992.
7. Paik, S., Bryant, J., Tan-Chiu, E., Romond, E., Hiller, W., Park, K., Brown, A., Yothers, G., Anderson, S., Smith, R., Wickerham, D. L., and Wolmark, N. Real-world performance of HER2 testing—National Surgical Adjuvant Breast and Bowel Project experience. J. Natl. Cancer Inst. (Bethesda), *94:* 852–854, 2002.
8. Roche, P. C., Suman, V. J., Jenkins, R. B., Davidson, N. E., Martino, S., Kaufman, P. A., Addo, F. K., Murphy, B., Ingle, J. N., and Perez, E. A. Concordance between local and central laboratory HER2 testing in the breast intergroup trial N9831. J. Natl. Cancer Inst. (Bethesda), *94:* 855–857, 2002.
9. Zujewski, J. A. "Build quality in"—HER2 testing in the real world. J. Natl. Cancer Inst. (Bethesda), *94:* 788–789, 2002.
10. Koscielny, S., Terrier, P., Spielmann, M., and Delarue, J. C. Prognostic importance of low c-erbB2 expression in breast tumors. J. Natl. Cancer Inst. (Bethesda), *90:* 712, 1998.
11. Koscielny, S., Terrier, P., Daver, A., Wafflart, J., Goussard, J., Ricolleau, G., Delvincourt, C., and Delarue, J. C. Quantitative determination of c-erbB-2 in human breast tumours: potential prognostic significance of low values. Eur. J. Cancer, *34:* 476–481, 1998.
12. Dittadi, R., Brazzale, A., Pappagallo, G., Salbe, C., Nascimben, O., Rosabian, A., and Gion, M. ErbB2 assay in breast cancer: possibly improved clinical information using a quantitative method. Anticancer Res., *17:* 1245–1247, 1997.
13. Ferrero-Pous, M., Hacene, K., Tubiana-Hulin, M., and Spyratos, F. Re: Prognostic importance of low c-erbB2 expression in breast tumors. J. Natl. Cancer Inst. (Bethesda), *91:* 1584–1585, 1999.
14. Ben-Levy, R., Paterson, H. F., Marshall, C. J., and Yarden, Y. A single autophosphorylation site confers oncogenicity to the Neu/ErbB-2 receptor and enables coupling to the MAP kinase pathway. EMBO J., *13:* 3302–3311, 1994.
15. Amundadottir, L. T., and Leder, P. Signal transduction pathways activated and required for mammary carcinogenesis in response to specific oncogenes. Oncogene, *16:* 737–746, 1998.
16. Janes, P. W., Daly, R. J., deFazio, A., and Sutherland, R. L. Activation of the Ras signalling pathway in human breast cancer cells overexpressing erbB-2. Oncogene, *9:* 3601–3608, 1994.
17. Sorlie, T., Perou, C. M., Tibshirani, R., Aas, T., Geisler, S., Johnsen, H., Hastie, T., Eisen, M. B., van de Rijn, M., Jeffrey, S. S., Thorsen, T., Quist, H., Matese, J. C., Brown, P. O., Botstein, D., Eystein Lonning, P., and Borresen-Dale, A. L. Gene expression patterns of breast carcinomas distinguish tumor subclasses with clinical implications. Proc. Natl. Acad. Sci. USA, *98:* 10869–10874, 2001.
18. Vogel, C. L., Cobleigh, M. A., Tripathy, D., Gutheil, J. C., Harris, L. N., Fehrenbacher, L., Slamon, D. J., Murphy, M., Novotny, W. F., Burchmore, M., Shak, S., Stewart, S. J., and Press, M. Efficacy and safety of trastuzumab as a single agent in first-line treatment of HER2-overexpressing metastatic breast cancer. J. Clin. Oncol., *20:* 719–726, 2002.
19. Cobleigh, M. A., Vogel, C. L., Tripathy, D., Robert, N. J., Scholl, S., Fehrenbacher, L., Wolter, J. M., Paton, V., Shak, S., Lieberman, G., and Slamon, D. J. Multinational study of the efficacy and safety of humanized anti-HER2 monoclonal antibody in women who have HER2-overexpressing metastatic breast cancer that has progressed after chemotherapy for metastatic disease. J. Clin. Oncol., *17:* 2639–2648, 1999.
20. Slamon, D. J., Leyland-Jones, B., Shak, S., Fuchs, H., Paton, V., Bajamonde, A., Fleming, T., Eiermann, W., Wolter, J., Pegram, M., Baselga, J., and Norton, L. Use of chemotherapy plus a monoclonal antibody against HER2 for metastatic breast cancer that overexpresses HER2. N. Engl. J. Med., *344:* 783–792, 2001.
21. Seidman, A. D., Fornier, M. N., Esteva, F. J., Tan, L., Kaptain, S., Bach, A., Panageas, K. S., Arroyo, C., Valero, V., Currie, V., Gilewski, T., Theodoulou, M., Moynahan, M. E., Moasser, M., Sklarin, N., Dickler, M., D'Andrea, G., Cristofanilli, M., Rivera, E., Hortobagyi, G. N., Norton, L., and Hudis, C. A. Weekly trastuzumab and paclitaxel therapy for metastatic breast cancer with analysis of efficacy by HER2 immunophenotype and gene amplification. J. Clin. Oncol., *19:* 2587–2595, 2001.